CHARACTERIZATION OF THE ABA PEAKING TYPE DYNAMIC DURING LONG TERM DROUGHT

by

Joel A. Mercado-Reyes

A Thesis

Submitted to the Faculty of Purdue University

In Partial Fulfillment of the Requirements for the degree of

Master of Science

Botany and Plant Pathology

West Lafayette , Indiana

December 2021

THE PURDUE UNIVERSITY GRADUATE SCHOOL
STATEMENT OF COMMITTEE APPROVAL

Dr. Scott McAdam, Chair
Department of Botany and Plant Pathology

Dr. Gyeong Mee Yoon
Department of Botany and Plant Pathology

Dr. Mike Mickelbart
Department of Botany and Plant Pathology

Approved by:
Dr. Christopher J. Staiger

Dedicated to Domingo Reyes-Noguera.

ACKNOWLEDGMENTS

I would like to acknowledge Amber H. Jannasch and Bruce R. Cooper for all the technical support during hormone data collection. As well as Cade Kane and Kean Kane for all the help and fun in the lab. Also, I would like to acknowledge Dr. Scott McAdam for providing me with the advice and support that guided me towards success.

TABLE OF CONTENTS

LIST OF FIGURES

ABSTRACT

Plants rely on diverse strategies to regulate water loss during drought. The phytohormone abscisic acid (ABA) is a critical mediator of stomatal closure during water stress in seed plants. Studies in conifers identified diverging strategies in long-term drought of ABA-mediated dynamics, particularly a peaking type dynamic during long term drought in some conifers. Few studies have reported this dynamic in angiosperms, and no study has revealed the mechanism driving declines in ABA levels as drought progresses in peaking type species. To understand peaking type dynamics, we exposed the model peaking type gymnosperm species *Callitris rhomboidea* and the highly drought resistant evergreen angiosperm *Umbellularia californica* to controlled long-term drought. We measured leaf water potentials (Ψ_l), stomatal conductance, ABA and the ABA catabolite phaseic acid (PA) levels in potted plants during a prolonged but non-fatal drought. We aimed to determine which of three potential drivers of peaking type dynamic were responsible for this response: (1) increased catabolism of ABA into PA at a threshold Ψ_l , (2) ABA export from the leaf is enhanced under drought, and (3) ABA biosynthesis ceases at a threshold Ψ_l. During long term drought, the evergreen angiosperm species *U. californica* demonstrated peaking type ABA dynamics like gymnosperms. In both species, PA levels did not increase significantly, in fact, PA levels tracked ABA levels, suggesting that ABA catabolism to PA may be a function of ABA levels. Girdling experiments to determine whether export from the leaf drove declines in ABA levels demonstrated that of the majority of ABA was likely converted to ABA glucose ester (ABA-GE), an inactive storage form of ABA, and exported from shoots during drought. Finally, by rapidly dehydrating branched collected at different timepoints during long-term drought we were able to determine that ABA biosynthesis is completely down regulated in

leaves that have been dehydrated beyond leaf turgor loss point. The decline in ABA levels in peaking type species appears conserved across seed plants and is mediated by high export rates in the form of ABA-GE. Future work should assess a more diverse selection of species as well as study long-term drought in less tolerant species to test whether ABA biosynthesis is deactivated in all species once Ψ_l declines below turgor loss point.

CHAPTER 1. CHARACTERIZATION OF THE ABA PEAKING TYPE DYNAMIC DURING LONG TERM DROUGHT

1.1 Introduction

Plant water use regulation relies on diverse species-specific strategies ranging from biomass allocation to dynamic physiological responses (Chaves et al., 2002). Water stress is an important driver of plant evolution and species distributions (Bowles, Paps, & Bechtold, 2021; Engelbrecht et al., 2007). In extreme cases water deficit leads to plant mortality (Brodribb, Powers, Cochard, & Choat, 2020). Extremely negative water potentials in the xylem causes the formation of embolism, which are air bubbles that disrupt the water transport system and subsequently lead to hydraulic failure and tissue desiccation (Brodribb et al., 2021; Brodribb & Cochard, 2009; Choat et al., 2012; Urli et al., 2013). A key adaptation in vascular plants that prevents declines in water potential and thus embolism formation when plants experience soil water deficit is the closure of stomata (Brodribb et al., 2021; Martin-StPaul, Delzon, & Cochard, 2017). Stomata are dynamic valves on the surface of leaves that open and close in response to environmental and endogenous signals (Hetherington & Woodward, 2003). During drought stomata close to prevent excessive evaporation. The closure of stomata during drought is a key adaptation to survive drought. Other strategies that allow plants to survive prolonged periods of drought include the evolution of xylem that is highly resistant of embolism formation (Larter et al., 2017; McAdam & Cardoso, 2019), and cuticles that are highly impermeable to water loss (Kerstiens, 1996). However, both of these strategies will only effectively prolong survival during drought if stomatal also close (Cochard, Pimont, Ruffault, & Martin-StPaul, 2020).

The mechanisms that drive stomatal closure during drought have long been debated. In seed plants the phytohormone abscisic acid (ABA) plays a critical role in closing stomata during

drought stress (Rodriguez-Dominguez et al., 2016; Tombesi et al., 2015). ABA is an essential plant hormone that plays a number of key roles in plant growth, development and function throughout the life cycle (Zhang et al., 2018). It regulates stress response, dormancy, and sex determination (Uknes & Ho, 1984). Arguably the most important role of ABA for seed plant survival is as a metabolic regulator of leaf gas exchange and transpiration during drought (Jones & Mansfield, 1970; Mittelheuser & van Steveninck, 1969). ABA levels increase during water deficit triggering rapid stomatal closure (Tardieu & Davies, 1992) . Seed plants rely on ABA mediated stomatal closure to ensure efficient stomatal closure during drought (McAdam & Brodribb, 2012). ABA biosynthesis is triggered by a loss of cell turgor as leaves dehydrate, with peak ABA biosynthesis occurring at a water potential that is close to turgor loss point (Ψ_{tlp}) in herbaceous species (Creelman & Mullet, 1991; McAdam & Brodribb, 2016; Pereira & Pallardy, 1989; Pierce & Raschke, 1980). However, few studies have characterized ABA dynamics after Ψ_{tlp} due to the tendency of herbaceous species experiencing catastrophic embolism at a water potential only slightly lower than Ψ_{tlp} (Skelton, Brodribb, & Choat, 2017).

In most herbaceous species, as well as tree species with relatively vulnerable xylem, as drought progresses ABA levels increase and continue to do so until embolism forms (Mittelheuser & van Steveninck, 1969). In contrast Brodribb and McAdam (2013) investigating ABA dynamics under long term drought in conifers discovered a diverging strategy in ABA dynamics. In the highly drought tolerant Cupressaceae species *Callitris rhomboidea* native to arid regions of southeastern Australia, stomata closed early in a drought stress driven by an increase in ABA levels (Brodribb & McAdam, 2013). However, once plants were dehydrated to –4 MPa, ABA levels stopped increasing, and over the subsequent 10 days of soil drought declined to prestress levels (Brodribb & McAdam, 2013). The reduction in ABA levels under long-term drought in *Callitris*

meant that stomata transitioned from closure being driven by ABA to closure being the result of a passive reduction in guard cell turgor, similar to the mechanism of stomatal closure under drought in ferns and lycophytes which have stomata that are insensitive to ABA (Cardoso, Randall, & McAdam, 2019; McAdam & Brodribb, 2012). This dynamic of ABA levels during drought was termed a "peaking type" ABA dynamic and has subsequently been well characterized in across the conifer phylogeny, being associated with the evolution of highly resistant xylem, defined as xylem requiring at least –4 MPa of tension to induce embolism in at least 50% of the xylem (Brodribb, McAdam, Jordan, & Martins, 2014). In conifer species from both the derived Cupressaceae (including species from both the Southern Hemisphere native Callitroid and sister Northern Hemisphere native Cupressoid clades) as well as Taxaceae have evolved peaking type ABA dynamics under controlled long-term drought. Peaking type ABA dynamics have been observed in the field in *Callitris intratropica* in which six months of no rainfall each year in the dry season in Northern Australia leads to a seasonal peaking-type ABA dynamic, such that at the end of the dry season stomata are closed yet ABA levels are as low as plants in the middle of the wet season when leaf water potentials are very high (Mcadam & Brodribb, 2015). There are only two studies so far which have documented a peaking-type ABA dynamic in angiosperm species, one in the extremely drought tolerant Central Australian native tree *Acacia aptaneura* (Fabaceae) (Nolan et al., 2017) and six species of arid adapted *Caragana* (Fabaceae) native to Inner Mongolia (Yao, Li, et al., 2021; Yao, Nie, et al., 2021). All of the angiosperm species in which a peaking type ABA dynamic during drought has been observed had highly resistant xylem to embolism formation and the water potential of peak ABA occurred between –3.5 and –4 MPa (Nolan et al., 2017; Yao, Li, et al., 2021; Yao, Nie, et al., 2021). From this observation we would hypothesize that highly resistant xylem is required for peaking type ABA dynamics across seed plants, and not just in

gymnosperms. A critical unknown about peaking type ABA dynamics is the mechanism driving this response of ABA under long term drought in species that have highly resistant xylem. Resolving this issue remains challenging because while highly resistant xylem has evolved independently in more than 130 species from 62 genera and 20 orders of seed plants (McAdam & Cardoso, 2019), there still remains no species with resistant xylem that has a sequenced genome. This lack of genetic information means that resolving the mechanistic question of how ABA levels decline under long term drought requires a physiological and biochemical approach.

There are a number of possible explanations for the peaking type dynamic in ABA levels during long term drought. Given that more than 90% of ABA synthesized under drought is catabolized into the primary catabolite for ABA, phaseic acid (PA) when plants are rewatered (Pierce & Raschke, 1981), the most likely explanation for the decline in ABA levels during long term drought in peaking type species is activated ABA catabolism. ABA is catabolized into PA by two biochemical steps encoded by cytochrome P450 *CYP707A* genes, the expression of these genes is upregulated when plants are rewatered during drought stress, and when plants are exposed to high humidity after acclimation to low humidity. ABA can also be reversibly inactivated by conjugation with UPD-glucose to a glucose ester form of the organic acid (ABA-GE) (Han, Watanabe, Shimada, & Sakamoto, 2020; Lim et al., 2005; Priest et al., 2006). ABA-GE can be stored in the vacuole (Han et al., 2020; Harris & Dugger, 1986), as well as exported from the leaf in the phloe

m stream (Ikegami, Okamoto, Seo, & Koshiba, 2009; Jeschke, Holobradá, & Hartung, 1997; Zeevaart & Boyer, 1984). ABA is converted to ABA-GE by a single step biochemical conversion catalyzed by two isoforms of β-glucosidase (Xu et al., 2012). Like an increase in catabolism to PA, there could be an enhanced rate of conjugation of ABA to ABA-GE under long

term drought that explains the decline in ABA levels. An additional explanation for the decline in ABA levels under long term drought could be by the ceasing *de novo* biosynthesis of ABA at a threshold water potential. While a loss of cell turgor is a well-described trigger for increasing the expression the gene encoding the rate limiting step in ABA biosynthesis in angiosperms, 9-*cis*-epoxycarotenoid deoxygenase (*NCED3* in *Arabidopsis*) (Qin & Zeevaart, 1999), only a relief of low cell turgor, via rehydration, is known to decrease the expression of this rate limiting step gene in the ABA biosynthetic pathway (McAdam, Sussmilch, & Brodribb, 2015). While never described before, the cessation of *de novo* ABA biosynthesis at a threshold negative water potential under drought would lead to a decrease in ABA levels that is independent of changes in the rate of ABA catabolism or conjugation. A final, but less likely explanation, is an increase in the rate of ABA export from the leaf via the phloem (Castro, Puertolas, & Dodd, 2019; López, Brossa, Gil, & Pita, 2015; Mitchell, McAdam, Pinkard, & Brodribb, 2017). However, given that the rate of phloem flux and ABA export rate is presumably very low during drought and non-existent when assimilation rate is negative, a common occurrence when stomata are closed (Sevanto, 2014).

In this study we sought to discover the mechanism driving declines in ABA levels under long term drought in peaking type seed plants. We conducted experiments on two species, the model system in which peaking-type ABA dynamics was first described, the gymnosperm species *Callitris rhomboidea* (Cupressaceae) and the highly drought resistant evergreen angiosperm species *Umbellularia californica* (Lauraceae) native to coastal forests and the foothills of the Sierra Nevada on the West Coast of North America. Water potentials, stomatal conductance, and ABA and PA levels were measured in potted plants of each species through a prolonged drought treatment until a non-fatal leaf water potential was reached to characterize ABA dynamics. We tested three hypotheses to determine the driving force behind the peaking type response: (1)

increased catabolism of ABA into PA occurs at a threshold water potential, (2) export of ABA out of the leaves is enhanced under drought, and/or (3) a cessation of ABA biosynthesis, driven by osmotic adjustment or turgor loss, is the major driver behind the declines in ABA level under long term drought. To assess catabolism driving the response we measured PA levels through the experiment. The role of export was assessed by girdling branches, in theory, accumulation of ABA and catabolites should be observed in leaves given that export is a mayor driver of decreasing levels of ABA in later stages of drought. And finally, to assess ABA biosynthesis being down regulated we designed a novel technique based on rapid bench dehydration as an alternative to gene expression in the absence of an available genome to assess the ability of shoots to rapidly synthesize ABA during short term drought.

1.2 Materials and Methods

1.2.1 Plant Material

Individuals of *Callitris rhomboidea* R. Br. ex Rich. & A. Rich. (Cupressaceae) and *Umbellularia californica* (Hook. & Arn.) Nutt. (Lauraceae) were potted in a mix of Indiana Miami topsoil, ground pine bark and sand at a 0.5:1:0.5 ratio. All species were grown from seed and the age of each species at the start of the experiment were three and five years of age, respectively. The plants were grown at Purdue University under controlled glasshouse conditions with approximately 12h natural light supplemented with LED lighting (16h day, 8h night; Illumitex Power Harvest I4, TX, USA) that provided a minimum photon flux at bench level of 150 μmol quanta m^{-2} s^{-1}. Under well-watered conditions, plants received daily watering and complete liquid nutrients (Miracle-Gro® Water-Soluble All Purpose Plant Food, The Scotts Company LLC, OH, USA) once every month. Glasshouse temperatures were set at 28 ºC during the day and 22 ºC

during the night. Air circulation fans in the glasshouse ensured continual air circulation, reducing boundary layer conductance.

1.2.2 Transpiration and hormone levels during drought

To measure daily whole plant transpiration pots were enclosed in a black plastic bag and covered in aluminum foil secured around the stem with a reversible cable tie to eliminate evaporation from the soil medium. During drought pots were weighted (Mettler Toledo, OH, USA) 30 minutes before and after solar midday. Drought was initiated by withholding water. Leaf samples for water potential determination and foliage hormone analysis were collected 30 minutes after solar midday after final weights were taken. Samples were wrapped in a moist paper towel then aluminum foil and placed inside a ziplock bag and then a cooler for transportation to the lab. Water potential was measured using a Scholander pressure chamber (PMS Instrument Company, OR, USA) and microscope for accurate determination of balance pressure, by slowly pressurizing and depressurizing the chamber. After measuring leaf water potential, a subsample of tissue was then taken for hormone analysis (see below). Upon reaching the most negative non-lethal leaf water potential determined from when signs of leaf death occurred under a prolonged drought for each species (-6 MPa for *C. rhomboidei* and -6 MPa for *U. californica*) plants were re-hydrated to full soil water capacity and measured daily until rates of transpiration had returned to pre-drought levels (approx. 5 days after re-hydration). Total plant foliage area was determined at the end of the experiment. In *U. californica* leaf area was calculated by scanning leaves (Epson Perfection V39 Scanner, Epson America, Inc., CA, US) and quantifying leaf area using the Fiji software (Schindelin et al., 2012). A mean individual leaf area was determined from these images and this value (12.68 cm^2) was used to adjust total plant leaf area during the experiment to account for leaves periodically harvested for water potential and foliage hormone analysis. In *C. rhomboidea*

leaf area was calculated from the ratio of dry weight to leaf area. Whole plant shoot area was harvested and dried to completeness at 70°C for 48h, after which it was weighed. Total leaf area was calculated from the ratio of dry mass to leaf area (70.80 $cm^2\ g^{-1}$) determined from samples that were scanned to determine projected area and weighed after drying to completeness. In *C. rhomboidea* a mean area of sample collected for water potential and hormone analysis was determined from 10 random samples (~2.86 cm^2). Like in *U. californica* this mean sample area was used to correct whole plant leaf area for declines due to sampling. Temperature and relative humidity measurements were recorded every 10 min using a HOBO MX2301A Data Logger (Onset Computer Corporation, MA USA), suspended at plant height in the glasshouse (Figures 1 and 2). The gravimetric determination of whole plant water loss was then used to calculate whole plant stomatal conductance by calculating whole plant transpiration (*E,* mol $m^{-2}\ s^{-1}$) using equation 1 and the leaf area determined above.

$$E = \frac{moles}{m^2 \cdot s} \quad (1)$$

Mean vapor pressure difference of the atmosphere (VPD) was for the hour during which whole plant transpiration was measured using equation 2.

$$VPD = (610.7 * 10^{\frac{7.5*T}{237.3+T}}) * \frac{(100-RH)}{100} \quad (2)$$

Where T is mean air temperature and RH is relative humidity for the duration of the transpiration measurements.

Whole plant stomatal conductance (g_s) was then calculated from E and VPD using equation 3:

$$g_s = \frac{E}{VPD \times P_{atm}} \quad (3)$$

Where P_{atm} is atmospheric pressure. We assumed negligible boundary layer conductance due to the constant air circulation in the glasshouse, and that leaf temperature approximated air temperature.

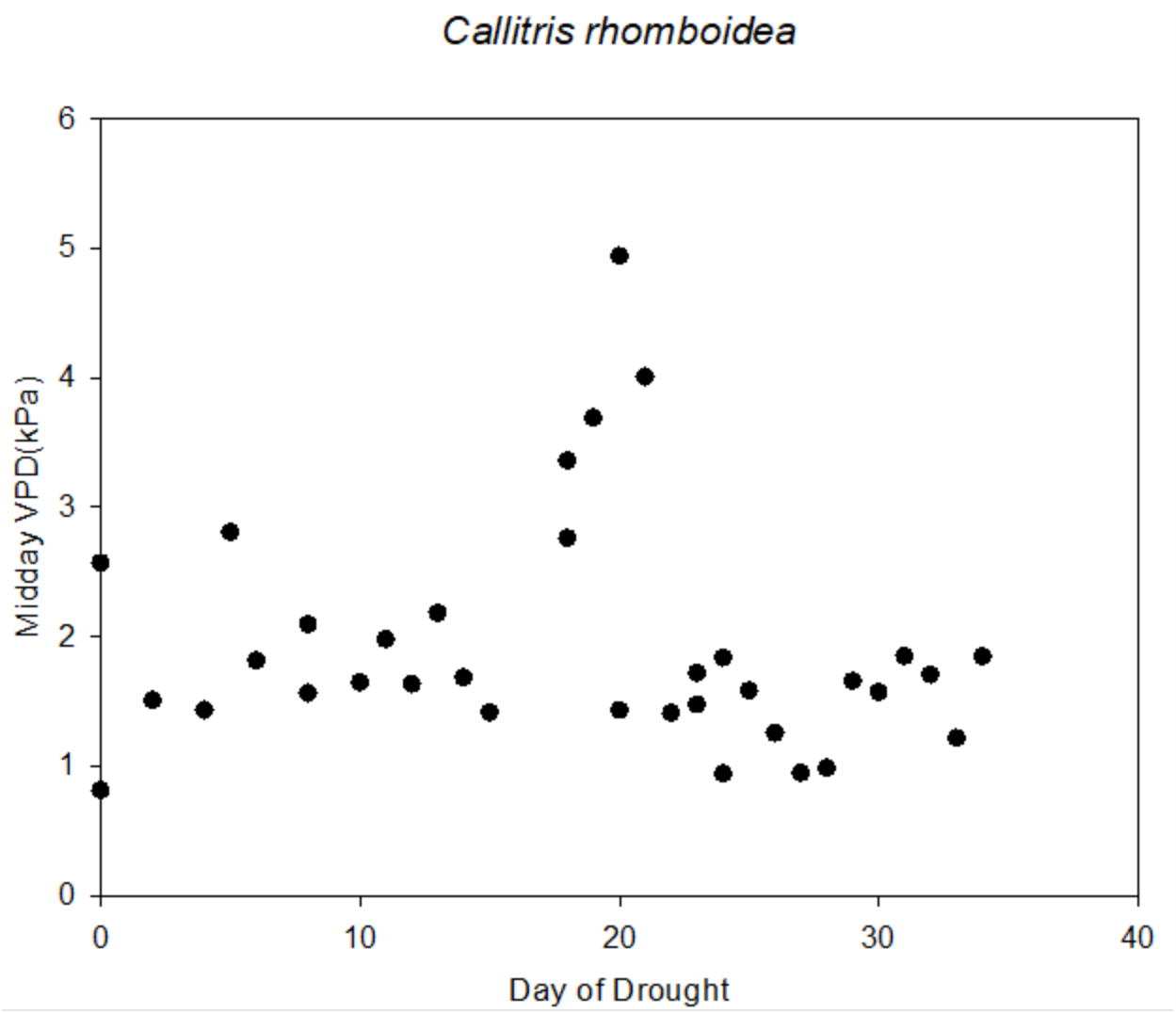

Figure 1. Midday vapor pressure deficit across time for the duration of drought stress in *Callitris rhomboidea.*

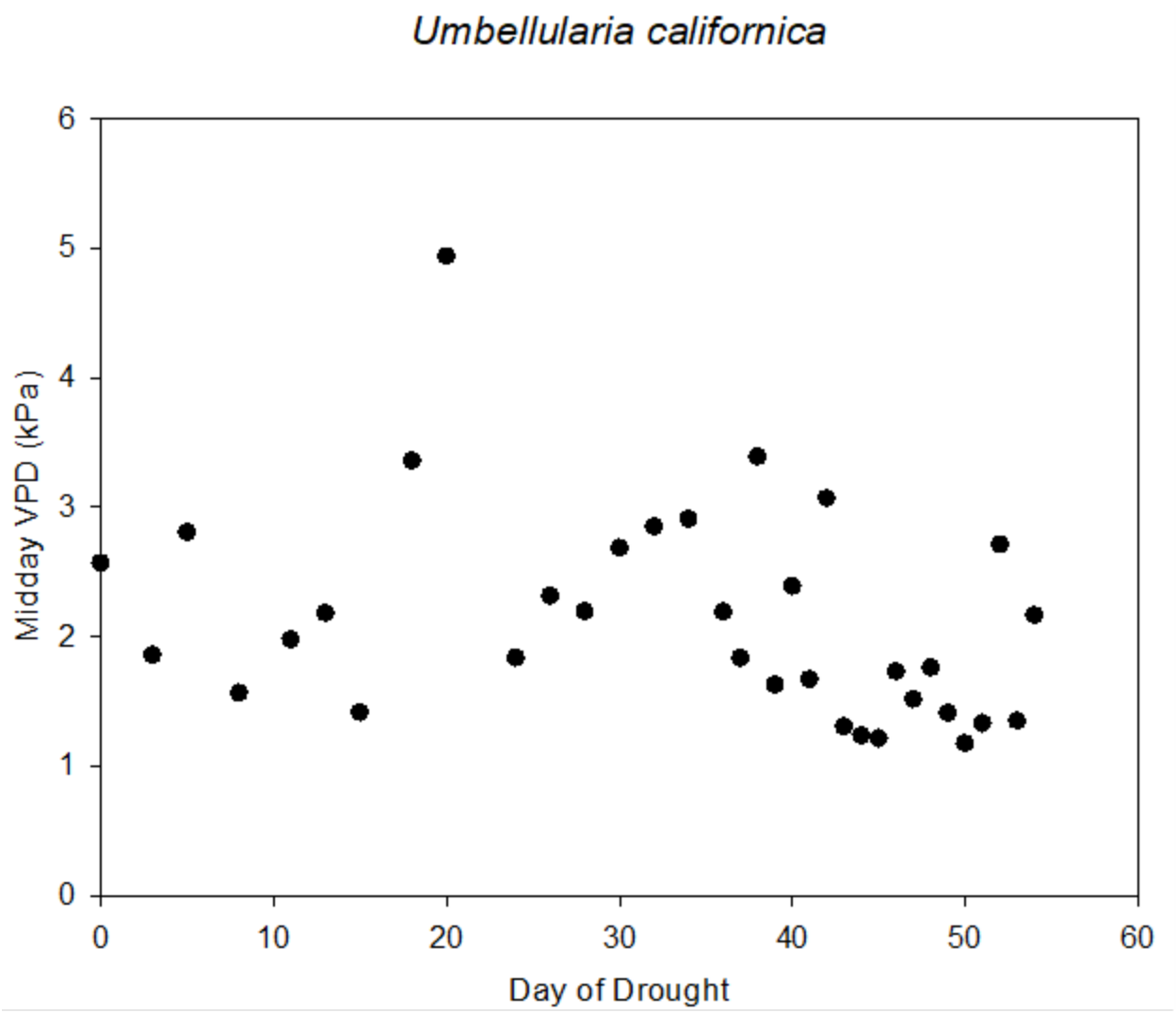

Figure 2. Midday vapor pressure deficit across time for the duration of drought stress in *Umbellularia californica.*

1.2.3 The effect of girdling on hormone levels during drought

To test for an effect of reduced phloem export during drought on foliage hormone levels, prior to drought a single, large branch on each individual of *C. rhomboidea* was girdled. Individual branches of *U. californica* were not sufficiently large or had enough leaves to be able to conduct the experiment in this species. Branches were girdled by carefully removing two to three centimeters of periderm just above the intersection of the branch and the main, leading stem. Samples from girdled and non-girdled branches were harvested concurrently to determine leaf water potential using a Scholander pressure chamber and collect a subsample for hormone quantification.

1.2.4 Rapid bench dehydration to assess ABA biosynthetic capacity.

A novel method was developed to test for the capacity of leaves to synthesize ABA. This method relies upon the well described effect of rapid dehydration being able to induce ABA biosynthesis in leaves (Jones & Mansfield, 1970; Mittelheuser & van Steveninck, 1971; Tardieu & Davies, 1992). In seed plants a reduction in turgor triggers the biosynthesis of ABA. Here branches were excised from individuals of each species at cardinal timepoints prior to water stress imposition and 10 days after peak ABA levels). To test whether tissue was capable of ABA biosynthesis branches were excised under water and rehydrated overnight. The following morning branches were dehydrated on a bench until a lethal threshold water potential was reached. Samples from the drying branches were collected periodically to determine leaf water potential and foliage ABA levels. Whole branch weight and laboratory environmental data were collected through time

to calculate the rate of water loss from branches and to ensure no differences in VPD occurred during the experiment.

1.2.5 Quantifying foliage Abscisic Acid (ABA), Phaseic Acid (PA) and ABA-Glucose Ester (ABA-GE).

Samples for hormone quantification were processed following a protocol of McAdam (2015). A subsample (around 100-300 mg) of each leaf collected as described previously was weighted (±0.0001g, OHAUS Corporation, NJ, USA) and covered with a cold (-20ºC) solution of 80% methanol in H_2O (v v^{-1}) containing 250 mg l^{-1} of butylated hydroxytoluene (BHT) as an antioxidant. Samples were chopped into fine pieces and stored at -20ºC. Samples were then homogenized (Bio-Gen PRO200 Homogenizer, PRO Scientific Inc, CT, US) and 15 µl of a solution containing 15 ng of [$^2H_6$] ABA and [$^2H_3$]PA and [$^2H_5$] ABA-GE (OlChemim Ltd, Czech Republic), and stored at 4 ºC overnight to allow the compounds to extract and the plant material to settle. Aliquots of approximately 6 mL of the supernatant were transferred to amber glass vials and dried to completeness in a vacuum sample concentrator (Labconco, MO, USA). To measure ABA-GE levels, we modified the extraction method to hydrolyze the conjugation by adding 3mL of 7M NaOH, heating for 3hs at 100 ºC. The pH of each sample was then measured and 20µL of 10M HCl were added to balance the pH. The hydrolyzed ABA was then separated from the solution by washing the solution with 200µL of dimethyl ether, collecting the ether phase, and allowing the solution to dry. Hormones were then resuspended in 200 µl of 2% acetic acid and 10% acetonitrile in H_2O (v v^{-1}). Each sample was then centrifuged at 14800 RPM for 3 minutes and a 100 µl aliquot was taken for analysis. ABA and PA levels with the respective internal standards were quantified using an Agilent 6460 series triple quadrupole LC/MS (Agilent, CA, USA) fitted with an xBridge HPLC column (C18, 2.1 x 100 mm, 3.5 µm, Waters Corporation, MA, USA). Solvents used were

2% acetic acid in H_2O (v v^{-1}, Solvent A) and acetonitrile (Solvent B) at a flow of 0.3mL min^{-1}. The running gradient went from 90% Solvent A and 10% Solvent B to 5% Solvent A and 95% Solvent B at 5 minutes and then back to initial values. An aliquot of 10 µL of sample was injected. The LC/MS was operated in negative ion electrospray mode with the needle running at 3.5 kV. To detect each metabolite and respective internal standard we used selected reaction monitoring. We used an ion source temperature of 325 ºC and nitrogen as the desolvation gas flowing at 8 l min^{-1}. The tandem transitions were m/z 263.1 to 153, 204 and 219, for ABA; for [$^2H_6$]ABA the transitions monitored were m/z 269.1 to 159, 207 and 225. For PA, the tandem transitions were m/z 279.3 to 139.1 and 205; and m/z 282.3 to 142.1 and 208, for [$^2H_3$]PA. The cone voltage was 100V. For all transitions, the collision energy was 5V. Dwell time was set to 50 ms for each channel. Hormone levels were analyzed in the Agilent Quantitative Analysis software. Quantification was done using the m/z 263.1 to 153 and corresponding labelled channel for ABA, and m/z 279.3 to 139.1 and corresponding labelled channel for PA. Finally, hormone levels in terms of ng per g fresh tissue weight was calculated as the ratio of endogenous to labelled hormone peak areas, multiplied by the amount labelled ABA added to the sample (in all cases 15 ng), divided by the fresh weight of the sample collected.

1.2.6 Pressure-Volume Curves

Pressure-volume curves to test for osmotic adjustment in response to long term drought were generated for both species prior to drought and in leaves collected from the same plants that had experienced long-term drought sufficient to reduce ABA levels to initial levels measured prior to the drought. Curves were conducted following the well-established procedures detailed by Sack and Pasquet-Kok (Sack & PrometheusWiki contributors, 2010). In short, five individual leaves or leafy shoots from the same individual were collected and rehydrated overnight to a hydrated state

(full hydration was considered when initial water potential was greater than -0.05 MPa). Tissue was scanned to obtain hydrated area then leaves or shoots were dehydrated on the bench, and measurements of weight and water potential were periodically recorded as water potential progressively declined (Tyree & Hammel, 1972). Water potential at turgor loss point and full turgor was calculated from the P-V curves generated as the water potential at which the relationship between the inverse of relative water content and leaf water potential deviates from a linear regression.

1.2.7 Data Analysis

General additive models and standard errors were fitted for ABA levels, PA levels, and stomatal conductance using the gam() function in the MGCV package (Wood, 2011) of R software (v.4.0.5, R Core Team, 2018). ANOVA was perfomed for all comparisons using the aov() function, and significant interactions were determined using the TukeysHSD() funtion of the multcomp package (Hothorn, Bretz, & Westfall, 2008) in R software. Correlation analysis for ABA and PA levels was performed using the cor.test() funtion in R software. Graphs were generated using the Sigmaplot software (v.10, Systat Software, Chicago, IL, USA)

1.3 Results

1.3.1 Foliage ABA and leaf water potential dynamics during long-term drought

During a long-term drought, the evergreen angiosperm species *Umbellularia californica* displayed a peaking-type ABA dynamic. Prior to drought at a water potential of -0.07 MPa, mean foliage ABA levels were 714 ± 610 ng g^{-1} FW (± SE, Figure 3). As leaf water potential (Ψ_l) declined, ABA levels rose to a mean peak of 4924 ± 399 ng g^{-1} FW (± SE, Figure 3) once Ψ_l had reached to -3.1 MPa (Figure 3). As plants experienced more negative Ψ_l ABA levels gradually

declined, decreasing back to a mean of 1085 ± 598 ng g at a Ψ_l of -6.02 MPa (Figure 3). ABA levels decreased on average by 154 ng g^{-1} FW MPa^{-1} between -3.1 and -6.02 MPa. In the conifer species *Callitris rhomboidea*, we also observed the typical peaking-type response in foliage ABA levels to increasingly negative Ψ_l (Figure 4). With a mean initial ABA level prior to drought being 236 ± 108 ng g^{-1} FW (±SE), then increasing to a mean peak of 845 ± 77 ng g^{-1} FW (±SE) at -2.7 MPa. After ABA peaked, levels of the hormone declined by an average of 259 ng g^{-1} FW MPa^{-1} to 275 ± 132 ng g^{-1} FW (±SE) at -4.99 MPa (Figure 4). Evidence of leaf death and a lack of recovery in maximum photosynthetic rate following rewatering for both species occurred once Ψ_l declined less than -6 MPa (personal observations, unpublished data).

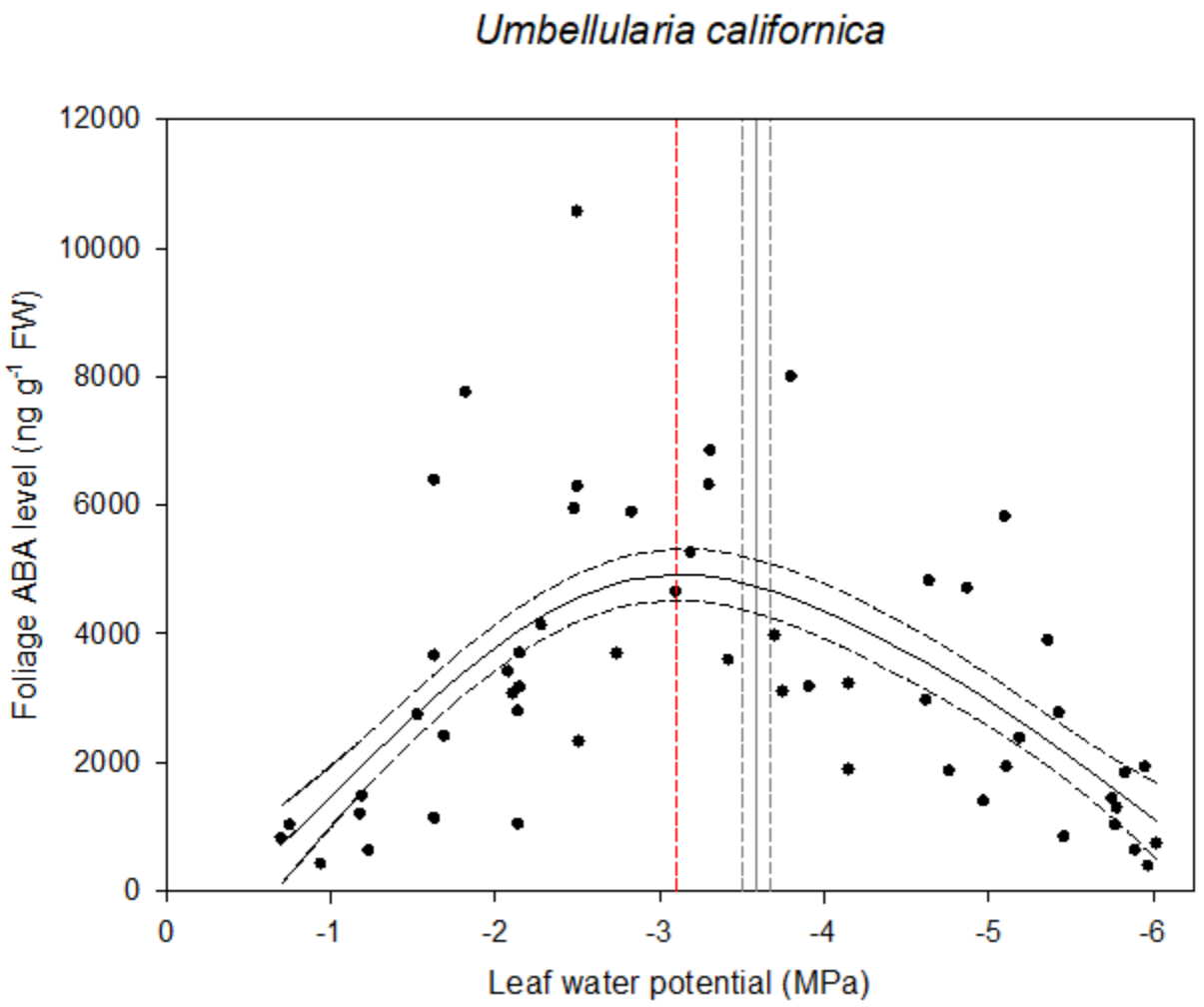

Figure 3. Foliage ABA levels during soil drought in the angiosperm *Umbellularia californica* (n =3). Generalized additive model (GAM) curves and standard errors are represented by solid and dashed lines, respectively. Mean leaf water potential (Ψ_l) at turgor loss point and standard errors are shown as gray solid and dashed lines, respectively. The red vertical line depicts the Ψ_l at peak foliage ABA level.

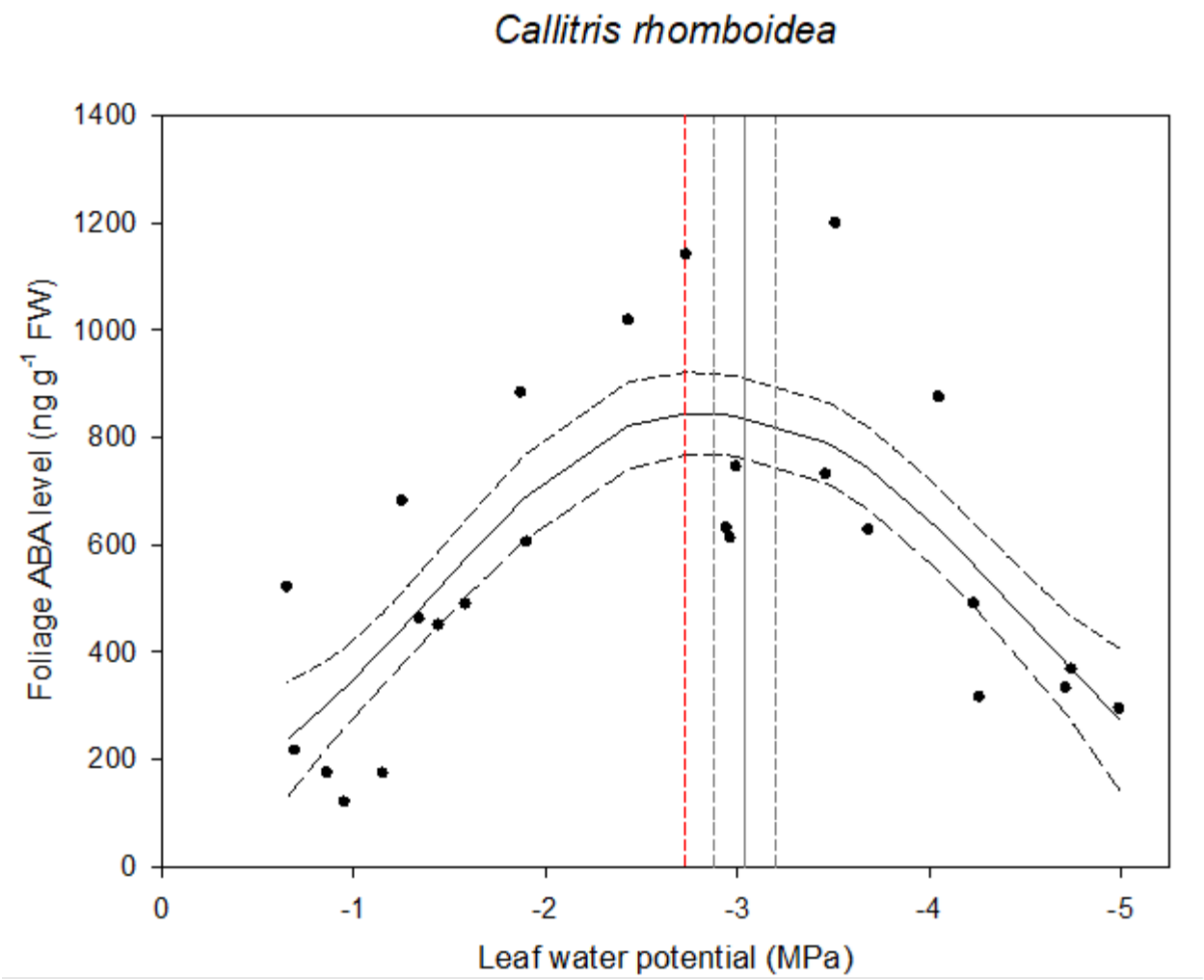

Figure 4. Foliage ABA levels during soil drought in the conifer *Callitris rhomboidea* (n=3). Generalized additive model (GAM) curves and standard error are represented by solid and dashed lines, respectively. Mean leaf water potential (Ψ_l) at turgor loss point and standard errors are shown as gray solid and dashed lines, respectively. The red vertical line depicts the Ψ_l at peak foliage ABA level.

In both species, we observed an exponential decline in whole plant stomatal conductance (g_s) as Ψ_l declined, with stomata being 83% and 99% shut once Ψ_l had declined to the Ψ_l at which peak levels of foliage ABA occurred in *U. californica* and *C. rhomboidea*, respectively (Figures 5 and 6). In *U. californica* mean (± SE) maximum g_s prior to drought was 0.0409 ± 0.002 mol m^{-2} s^{-1}, this exponentially declined to a minimum of 0.0042 ± 0.002 mol m^{-2} s^{-1} by -6.02 MPa (Figure 5). In *C. rhomboidea,* mean (± SE) maximum g_s prior to drought was 0.017 ± 0.001 mol m^{-2} s^{-1}, this declined to a minimum of 0.00026 ± 0.0013 mol m^{-2} s^{-1} by -6.02 MPa (Figure 6). Stomata remained closed for the duration of the drought in both species.

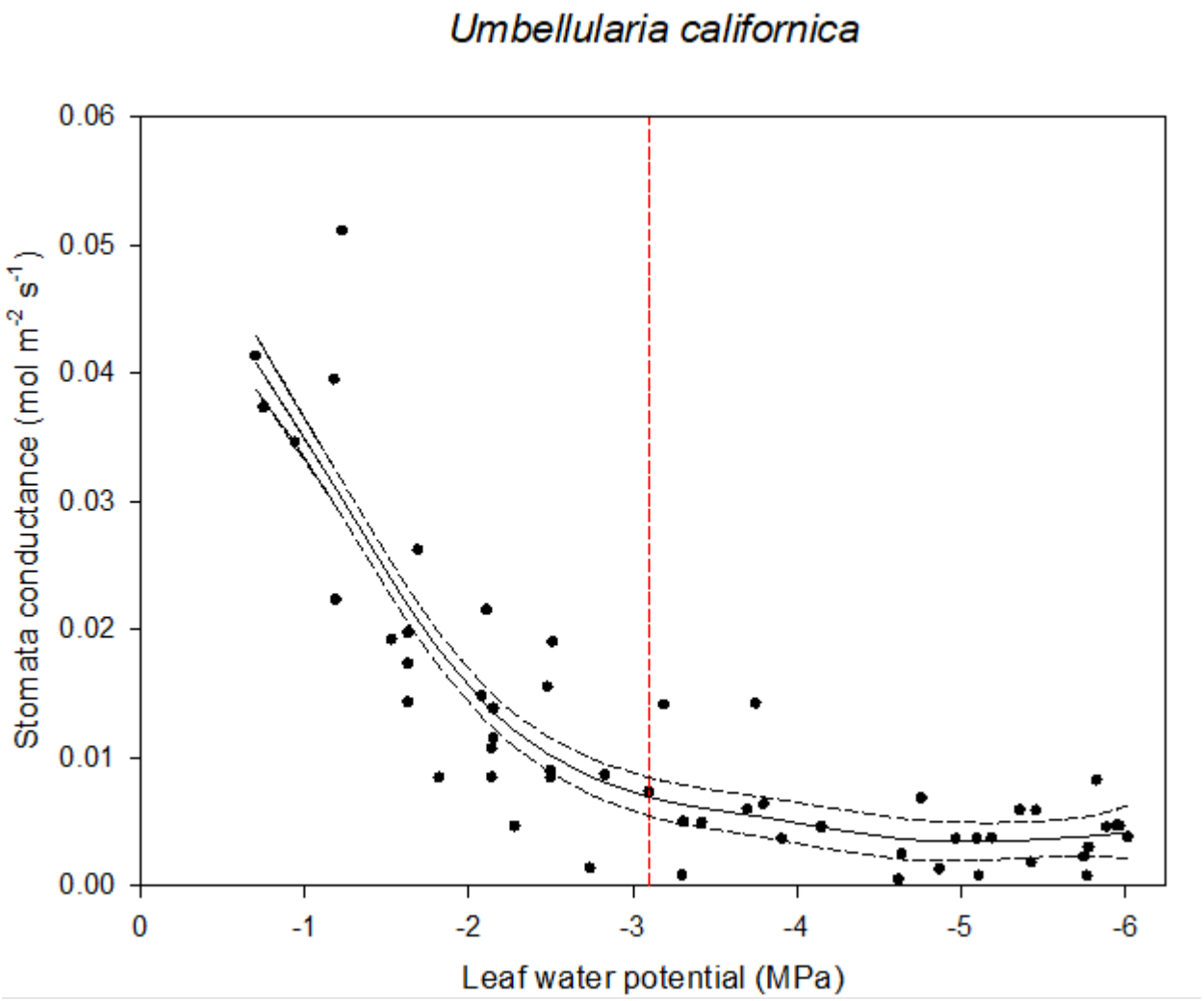

Figure 5. Whole plant stomatal conductance as leaf water potential (Ψ_l) declines during soil drought in the angiosperm *Umbellularia californica* (n=3). Generalized additive model (GAM) curves and standard errors are represented by solid and dashed lines, respectively. The vertical red line represents the Ψ_l at peak foliage ABA level.

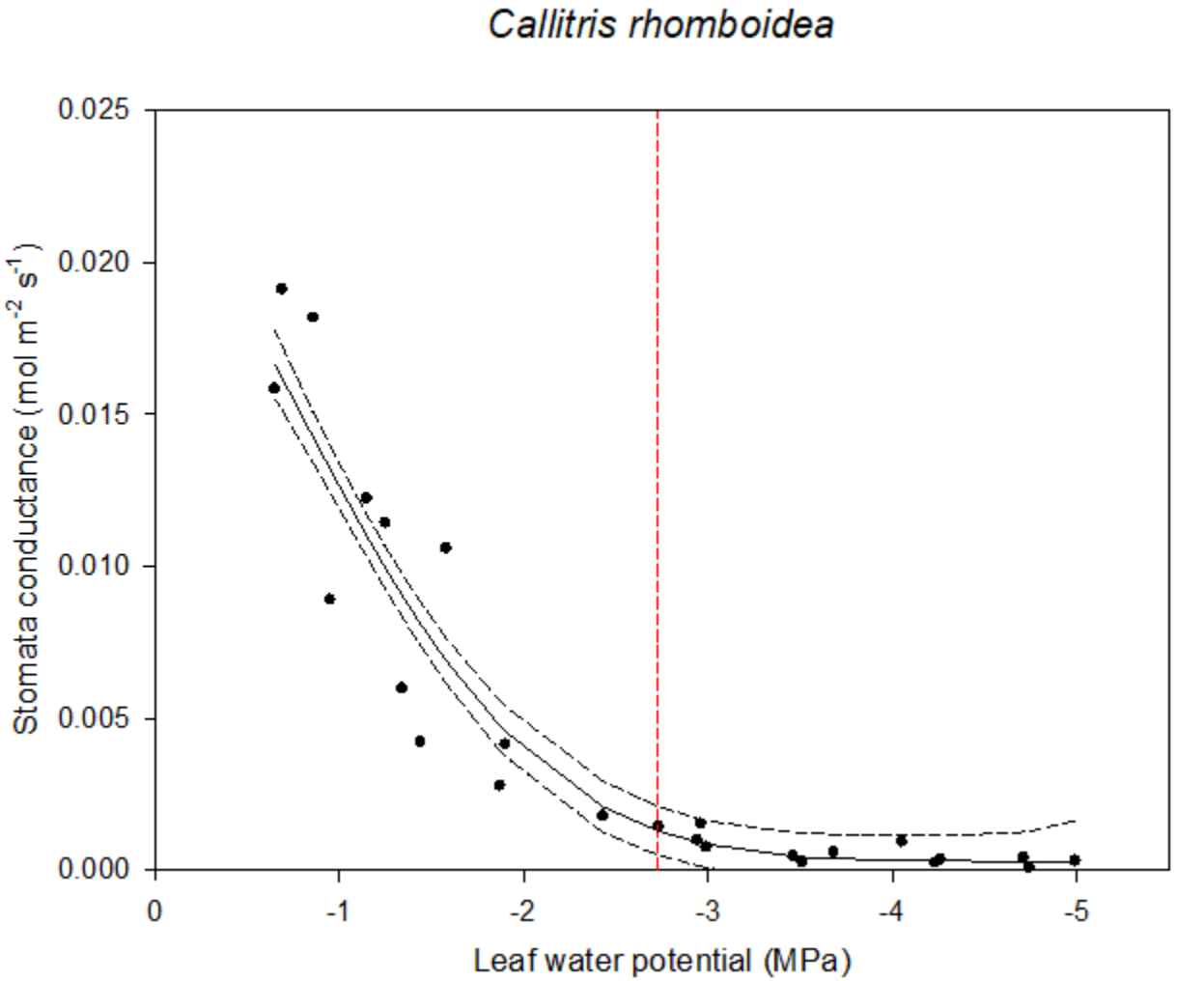

Figure 6. Whole plant stomatal conductance as as leaf water potential (Ψ_l) declines during soil drought in the conifer *Callitris rhomboidea* (n=3). Generalized additive model (GAM) curves and standard error are represented by solid and dashed lines, respectively. The vertical red line represents the Ψ_l at peak foliage ABA level.

1.3.2 Dynamics of the ABA catabolite phaseic acid during long term drought

During long term drought foliage phaseic acid (PA) levels were closely correlated with ABA levels in the angiosperm *U. californica* (*Pearson's* $r_{57} = 0.74$, $p < 0.0001$) while no significant correlation was observed in the conifer *C. rhomboidea* (*Pearson's* $r_{23} = 34$, $p = 0.09234$). In *U. californica* mean foliage PA levels were 292 ± 95 ng g^{-1} FW (± SE) at -0.07 MPa prior to the drought, then as Ψ_l decreased to -3.3 MPa foliage PA levels increased reaching a maximum of 969 ± 63 ng g^{-1} FW (±SE) (Figure 7). As drought progressed foliage PA levels declined in *U. californica* reaching a minimum of 545 ng g^{-1} FW at -6.02 MPa, at a rate of 166.51 ng g MPa^{-1} (Figure 7). Similarly, in the conifer *C. rhomboidea*, PA levels increased from a mean of 107 ± 104 ng g^{-1} FW at -0.65 MPa to a maximum of 504 ± 83 ng g^{-1} FW as water potentials decreased to -3.51 MPa (Figure 8). PA levels then decreased at a rate of 294 ng g^{-1} FW MPa^{-1} to 150 ± 133 ng g^{-1} FW (± SE) at -4.99 MPa.

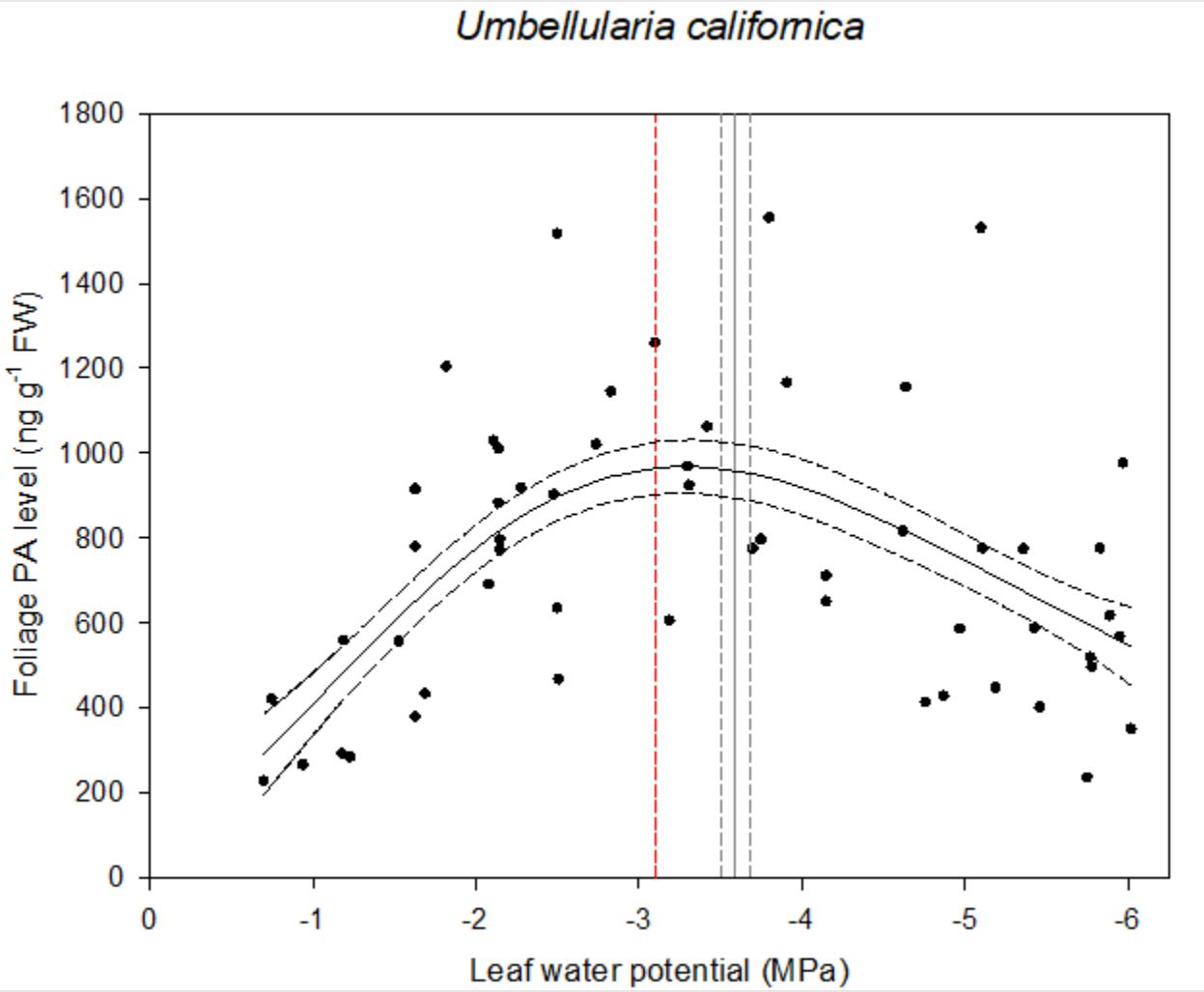

Figure 7. Foliage phaseic acid (PA) levels as leaf water potential (Ψ_l) declines during soil drought in the angiosperm *Umbellularia californica* (n =3). Generalized additive model (GAM) curves and standard errors are represented by solid and dashed lines, respectively. Mean Ψ_l at turgor loss point and standard errors are shown as gray solid and dashed lines, respectively. The red vertical line depicts the Ψ_l at peak foliage ABA level.

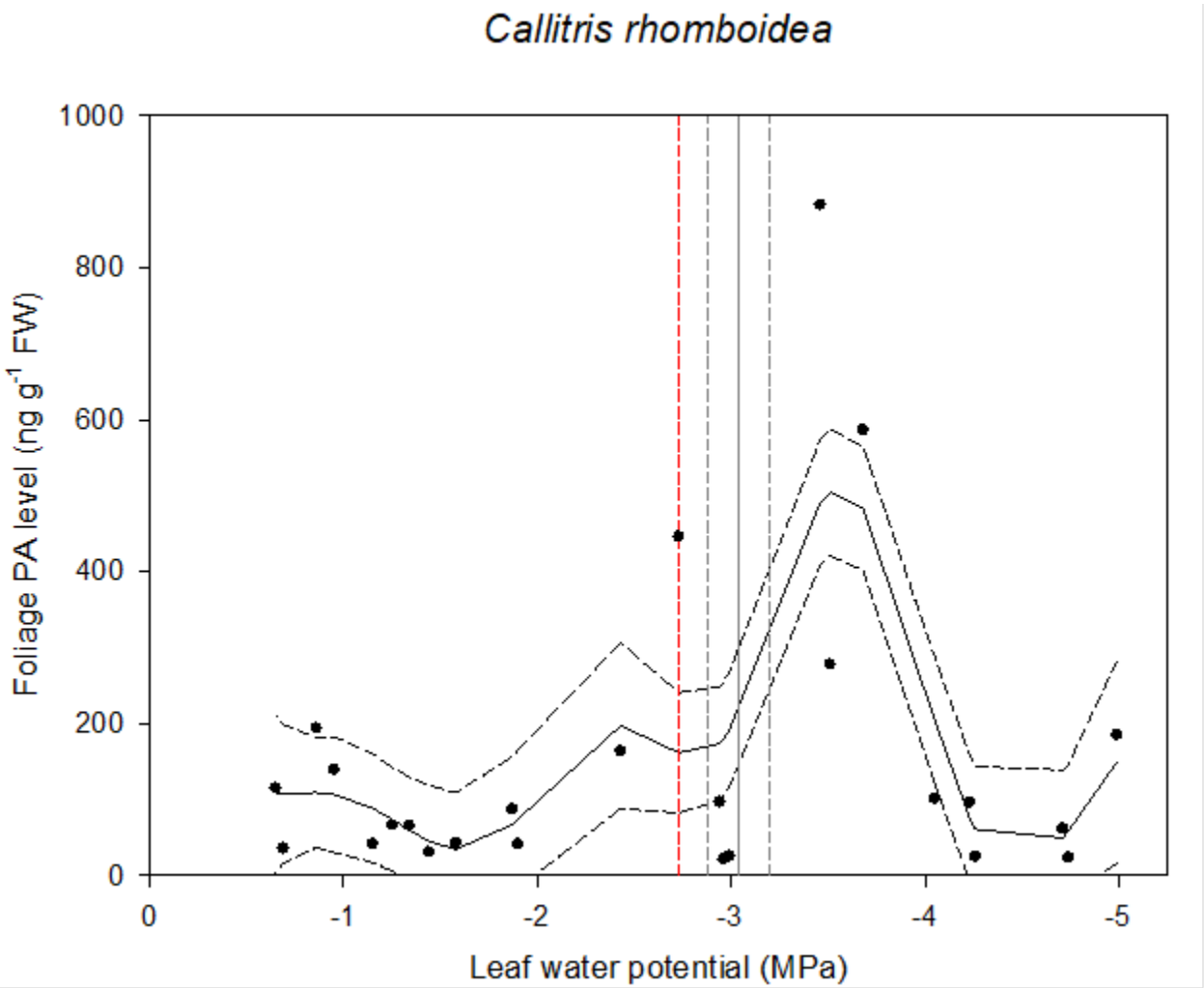

Figure 8. Foliage phaseic acid (PA) levels as leaf water potential (Ψ_l) declines during soil drought in the conifer *Callitris rhomboidea* (n=3). Generalized additive model (GAM) curves and standard errors are represented by solid and dashed lines, respectively. Mean Ψ_l at turgor loss point and standard errors are shown as gray solid and dashed lines, respectively. The red vertical line depicts the Ψ_l at peak foliage ABA level.

1.3.3 Girdling in *C. rhomboidea* has no influence on foliage ABA and PA dynamics during long term drought

In the conifer *C. rhomboidea* branch girdling had no effect on mean foliage ABA levels or dynamics during long term drought (Figure 9). Mean ABA levels in girdled branches of *C. rhomboidea* increased from 204 ± 104 ng g^{-1} FW at -0.59 MPa to 775 ± 84 ng g^{-1} FW at -3.16 MPa (Figure 9), this was similar to levels of ABA in un-girdled branches (t-test, $p = 0.3937$). Following the peak in foliage ABA levels, levels declined to a mean of 574 ± 112 ng g^{-1} FW at -4.88 MPa. Foliage PA levels in girdled branches of *C. rhomboidea* slightly increased with decreasing Ψ_l but no peaking behavior was observed in the girdled branches (Figure 10). Due to limited shoot material girdling was not possible in the angiosperm *U. californica*.

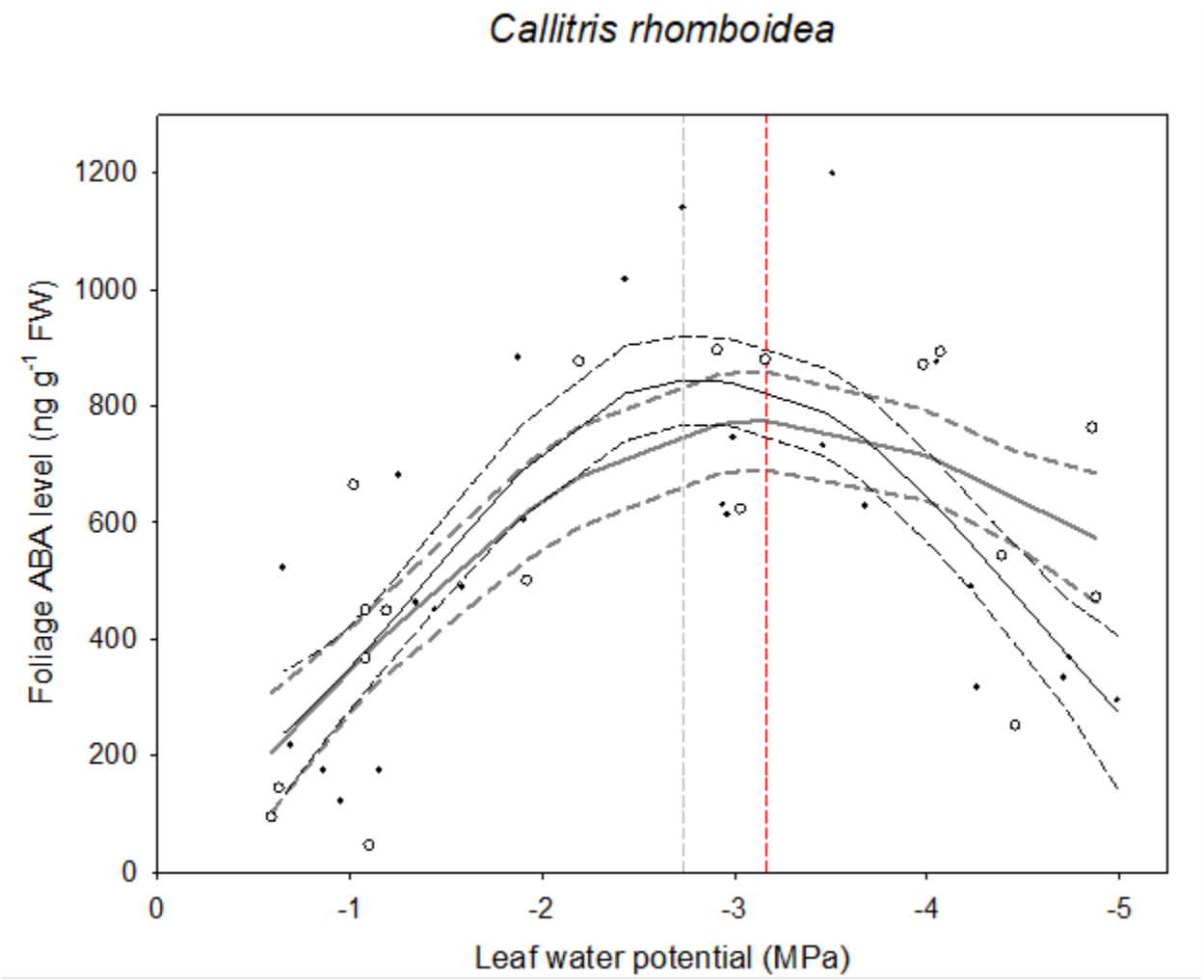

Figure 9. Foliage ABA levels as leaf water potential (Ψ_l) declines during soil drought in branches of *Callitris rhomboidea* that have been girdled (n=3, open circles, grey lines) or not (n=3, dark circles, black lines). Generalized additive model (GAM) curves and standard errors are represented by black solid and dashed lines for ungirdled branches and gray solid and dashed lines for girdled branches, respectively. Vertical red and grey dashed lines represent Ψ_l at peak foliage ABA level for girdled and ungirdled branches, respectively.

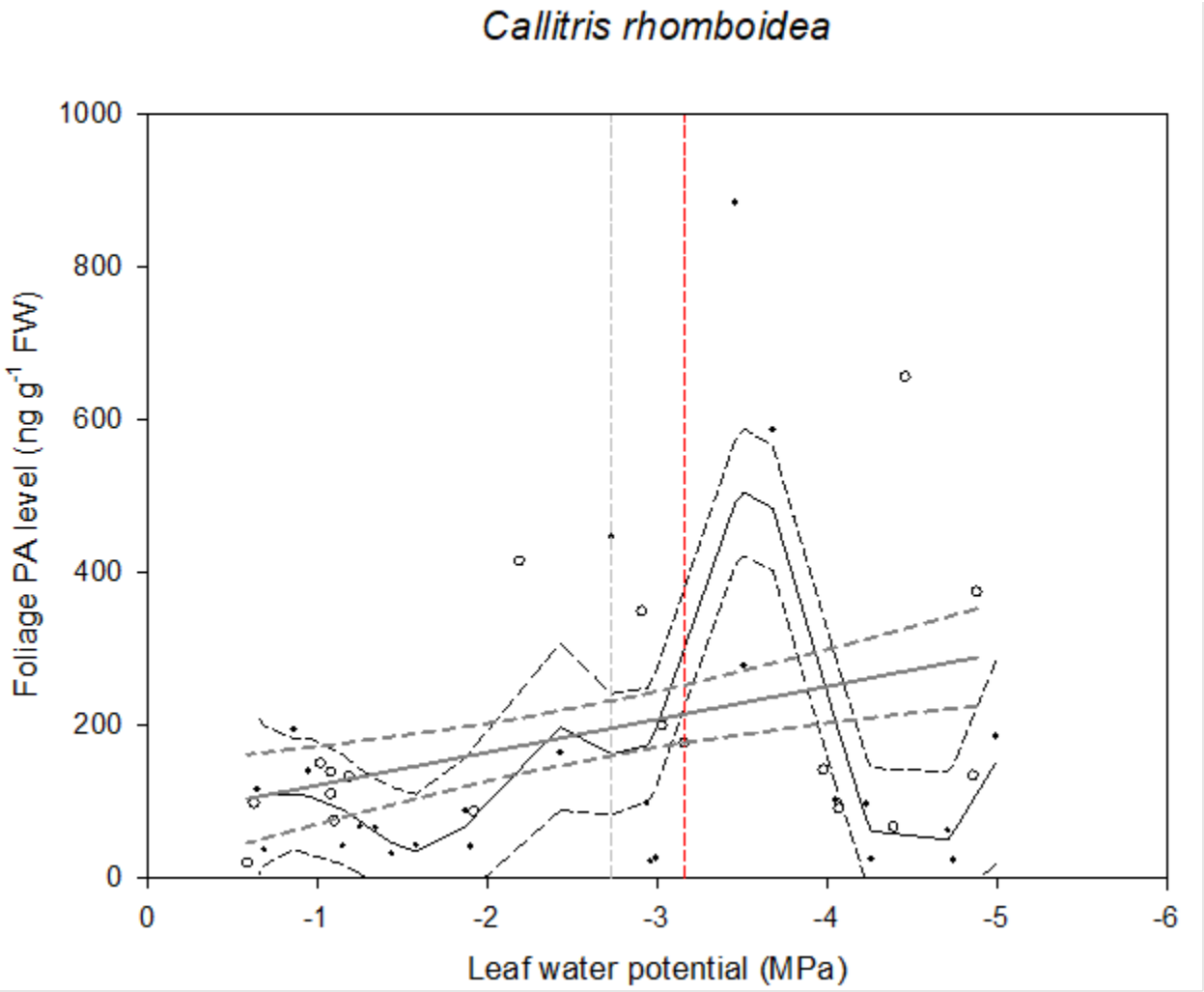

Figure 10. Foliage phaseic acid (PA) levels as leaf water potential (Ψ_l) declines during soil drought in branches of *Callitris rhomboidea* that have been girdled (n=3, open circles, grey lines) and ungirdled branches (n=3, dark circles, black lines). Generalized additive model (GAM) curves and standard errors are represented by black solid and dashed lines for ungirdled branches and gray solid and dashed lines for girdled branches, respectively. Vertical red and grey dashed lines represent Ψ_l at peak foliage ABA level for girdled and ungirdled branches, respectively.

1.3.4 The ability to synthetize ABA ceases under long term drought in angiosperms and conifers

In the angiosperm *U. californica,* we observed that rapid bench dehydration of never-before stressed branches triggers rapid and considerable accumulation of foliage ABA levels (Figure 11). In *U. californica* foliage ABA levels increased by 345 ng g^{-1} FW h^{-1} as branches were dehydrated on the bench (Figure 11). In contrast, in branches collected from plants under long-term drought at least 10 days after peak foliage ABA level, that were rehydrated overnight and then allowed to bench dehydrate, Ψ_l decreased rapidly while ABA levels remained low (less than 767 ± 92 ng g^{-1} FW, mean ± SE, Figures 9 and 10). Ψ_l in never-before stressed branches of *U. californica* which accumulated considerable levels of ABA on rapid dehydration decreased at a slower rate than for branches that were collected from plants that had experienced long-term drought, with WP at 3.25 h after the initiation of dehydration being of -0.50 MPa in never-before stressed branches and -2.47 MPa in branches collected from plants experiencing long-term drought that were not accumulating foliage ABA levels, respectively (Figure 12). Similarly, in the conifer *C. rhomboidea* foliage ABA levels increased in unstressed branches from 153 ± 103 ng g^{-1} FW to 1743 ± 304 ng g^{-1} FW at 6 h while post-peak branches displayed relative low levels of foliage ABA increasing from 90 ± 19 ng g^{-1} FW to just 225 ± 24 ng g^{-1} FW at 6 h (Figure 13). The relationship between Ψ_l and time in the respective branches was similar in both species, with Ψ_l in never-before stressed branches of the conifer *C. rhomboidea* decreasing at a slower rate than that of branches collected from plants under long-term drought in which ABA levels were initially low, and in which ABA levels did not considerable accumulate on rapid bench dehydration, with WP decreasing to -1.83 MPa in never-before stressed branches and -3.96 MPa in branches from plants under long-term drought at 6 h (Figure 14).

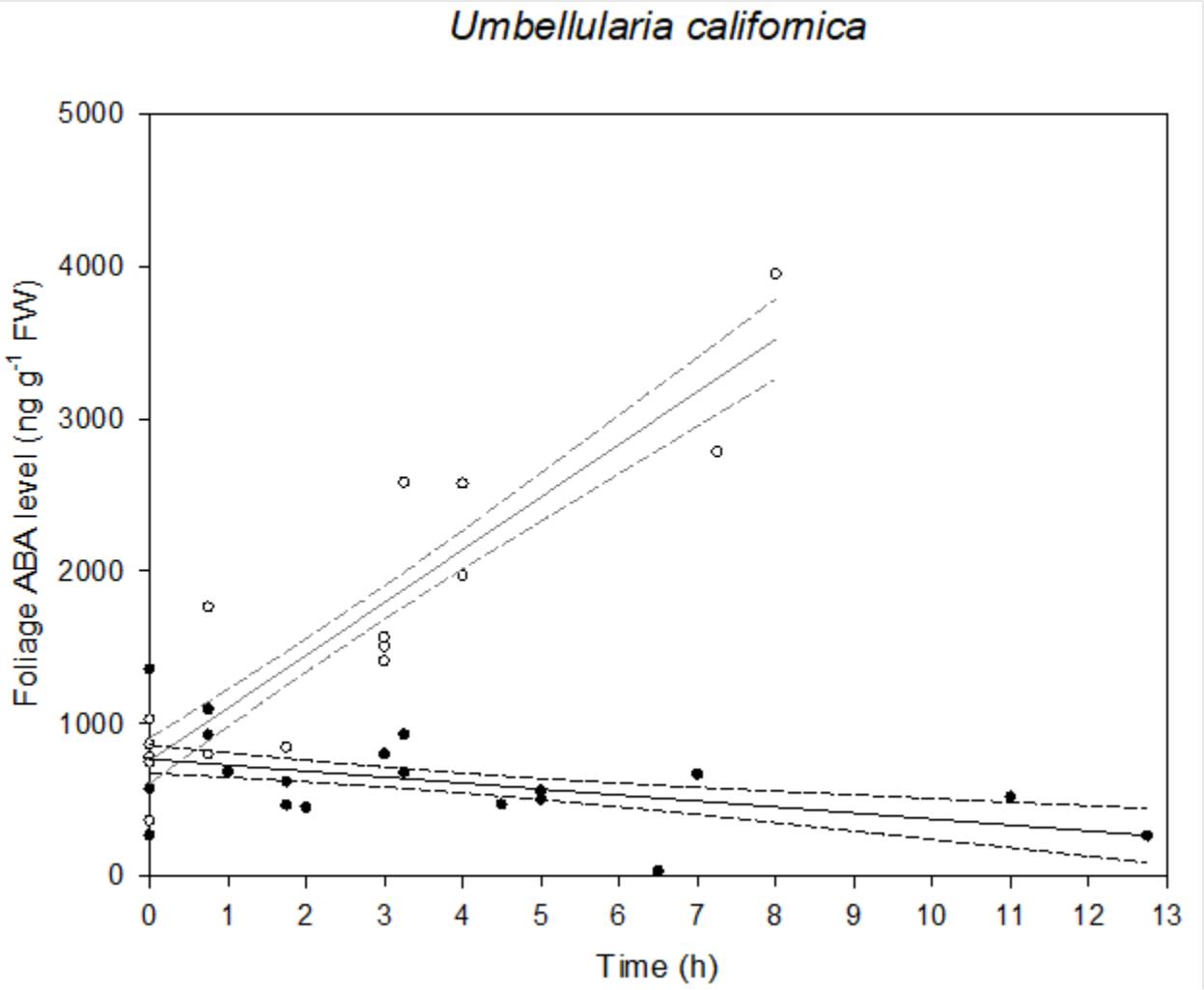

Figure 11. Foliage ABA levels in bench dried branches of the angiosperm *Umbellularia californica* that were fully hydrated at time 0. Branches were taken from plants that had never been stressed (open circles, gray regressions) or had experienced considerable soil drought having spent at least 10 days at a leaf water potential lower than when foliage ABA levels had peaked (solid line and closed circles). Generalized additive models (GAM) curves and standard errors are represented by solid and dashed lines, respectively.

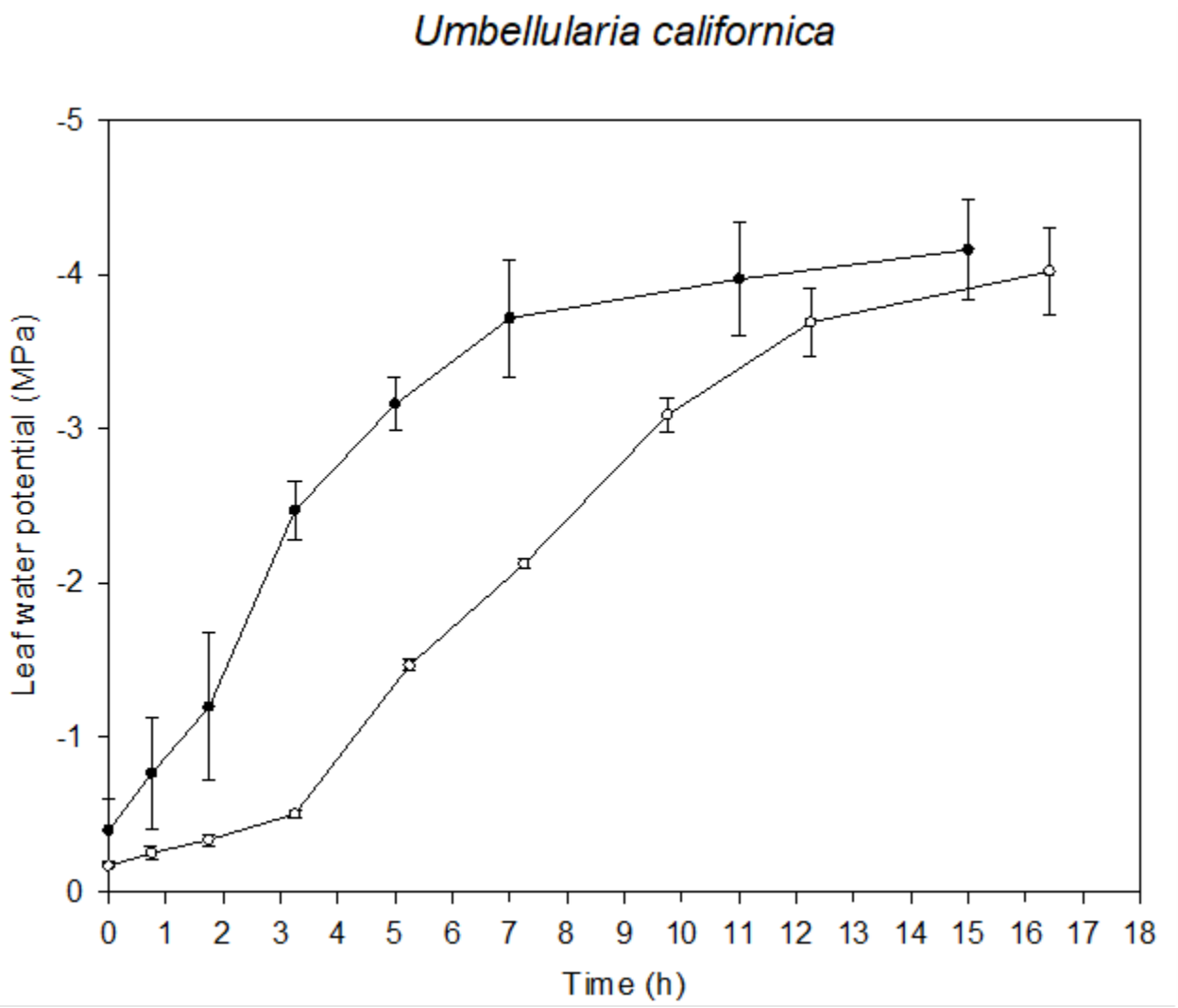

Figure 12. Mean leaf water potential (Ψ_l) through time in bench dried branches of the angiosperm *Umbellularia californica* (n=3, ±SE). Branches were taken from plants that had either never been stressed (open circles) or had experienced considerable soil drought having spent at least 10 days at a leaf water potential lower than when foliage ABA levels had peaked (closed circles).

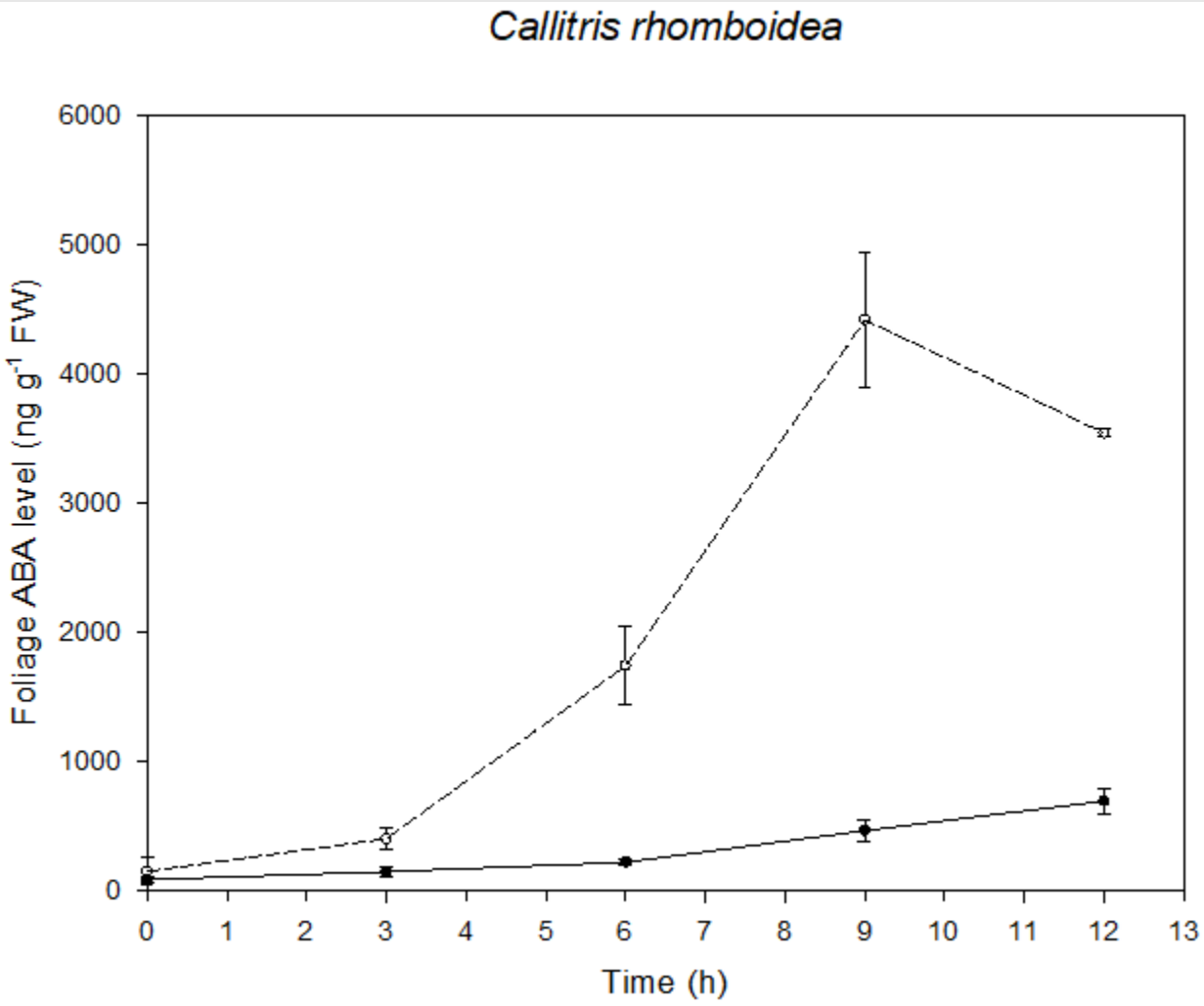

Figure 13. Mean foliage ABA levels in bench dried branches of the conifer *Callitris rhomboidea* that were fully hydrated at time 0 (n=3, ±SE). Branches were taken from plants that had never been stressed (open circles, dashed line) or had experienced considerable soil drought having spent at least 10 days at a leaf water potential lower than when foliage ABA levels had peaked (closed circles, solid line).

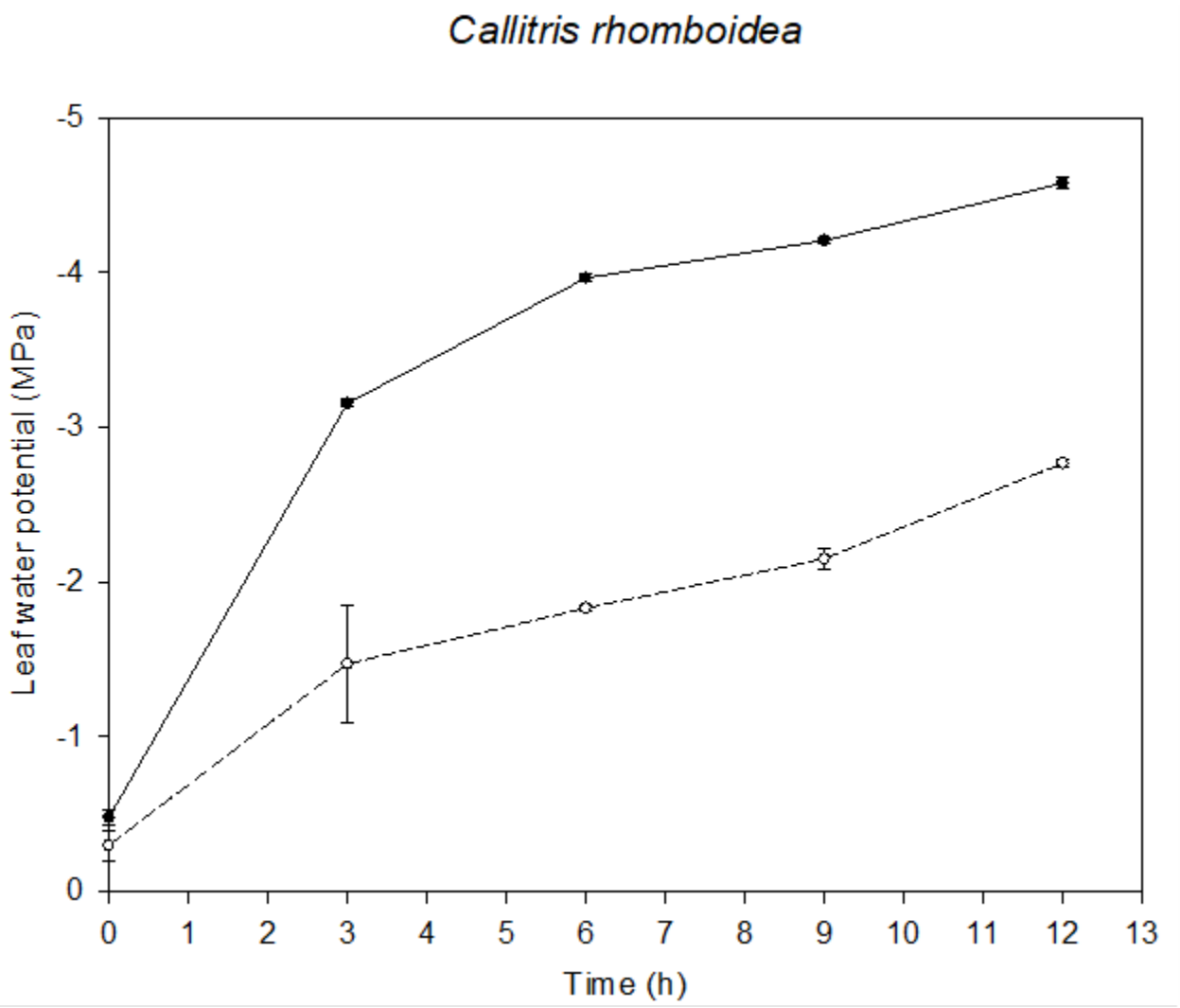

Figure 14. Mean leaf water potential (Ψ_l) over time in bench dried branches of the conifer *Callitris rhomboidea (*n=3, ±SE). Branches were taken from plants that had either never been stressed (open circles) or had experienced considerable soil drought having spent at least 10 days at a leaf Ψ_l lower than when foliage ABA levels had peaked (closed circles).

1.3.5 Osmotic adjustment during long term drought

In the angiosperm *U. californica* mean turgor loss point (Ψ_{tlp}) in never-before stressed plants was -3.66 ± 0.18 MPa (Figure 15). In leaves collected from plants approximately 10 days after peak ABA level, when Ψ_l had declined to -6 MPa, turgor loss point was not significantly lower than never-before stressed plants ($t_{5.06} = 1.2042$, $p = 0.2817$), with a mean Ψ_{tlp} of -3.58 ± 0.20 MPa. Similarly, in the conifer *C. rhomboidea*, mean Ψ_{tlp} in never-before stressed plants was -2.83 ± 0.34 MPa (Figure 16), which was not significantly different than mean Ψ_{tlp} in leaves of plants that had experienced drought for at least 10 days after peak ABA levels (-3.04 ± 0.16 MPa, $t_{7.98} = -1.69$, $p = 0.1296$) at a mean Ψ_l approximately -6 MPa. The turgor loss points of the two species were different for both prestressed and post peak timepoints (ANOVA, $p < 0.05$).

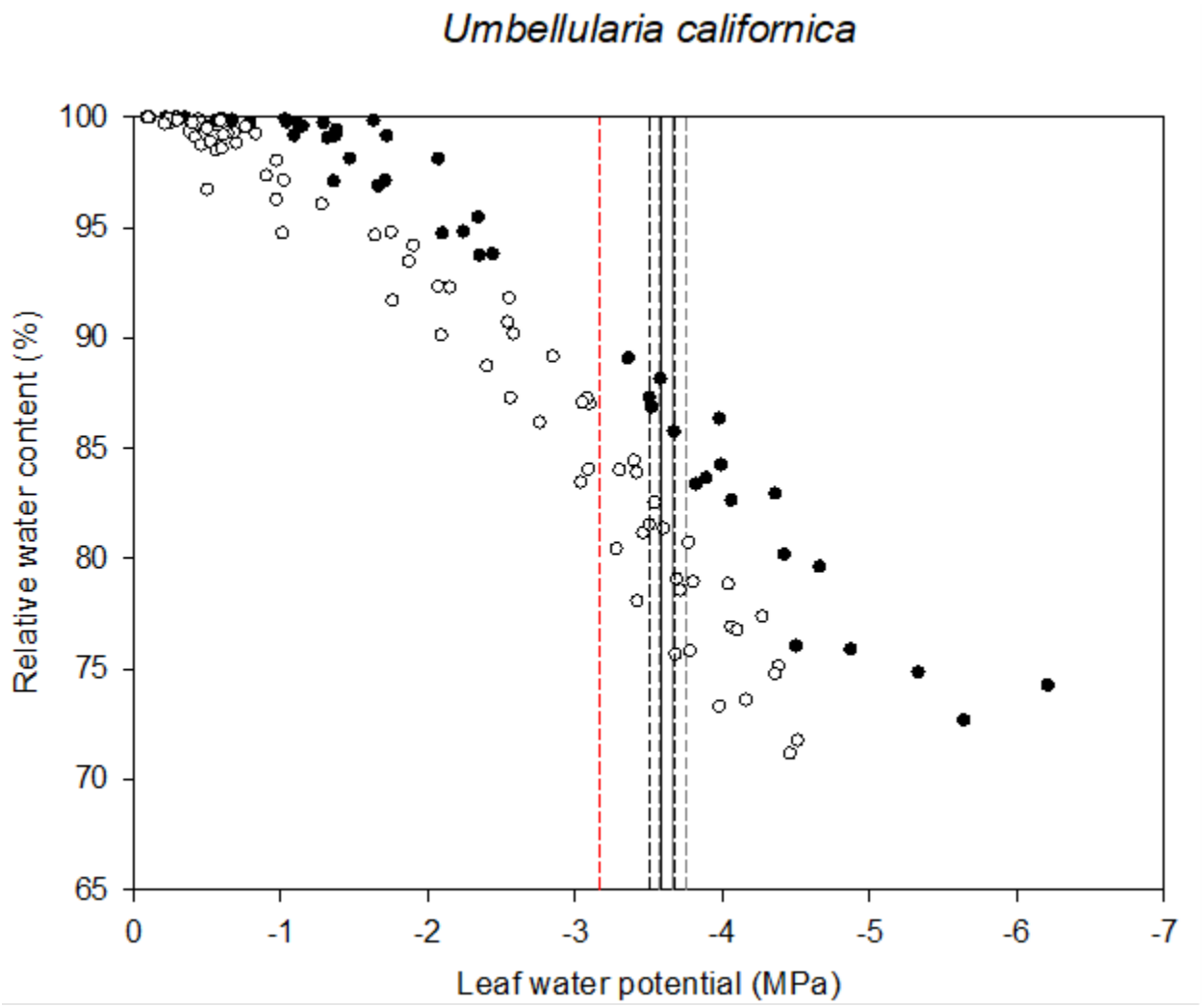

Figure 15. Relative water content as leaf water potential (Ψ_l) declines in leaves of the angiosperm *Umbellularia californica* (n=5) for never-before stressed plants and plants that had experienced long-term drought and at least 10 days at Ψ_l more negative than when peak foliage ABA level occurred (open and closed circles, respectively). Black vertical and dashed lines represent mean leaf water potential at turgor loss point (Ψ_{tlp}) and standard error for leaves collected from plants under long-term drought. Grey solid and dashed vertical lines represent mean Ψ_{tlp} and standard error for leaves of never-before stressed plants. Red dashed lines depict the Ψ_l at which peak foliage ABA levels occurred.

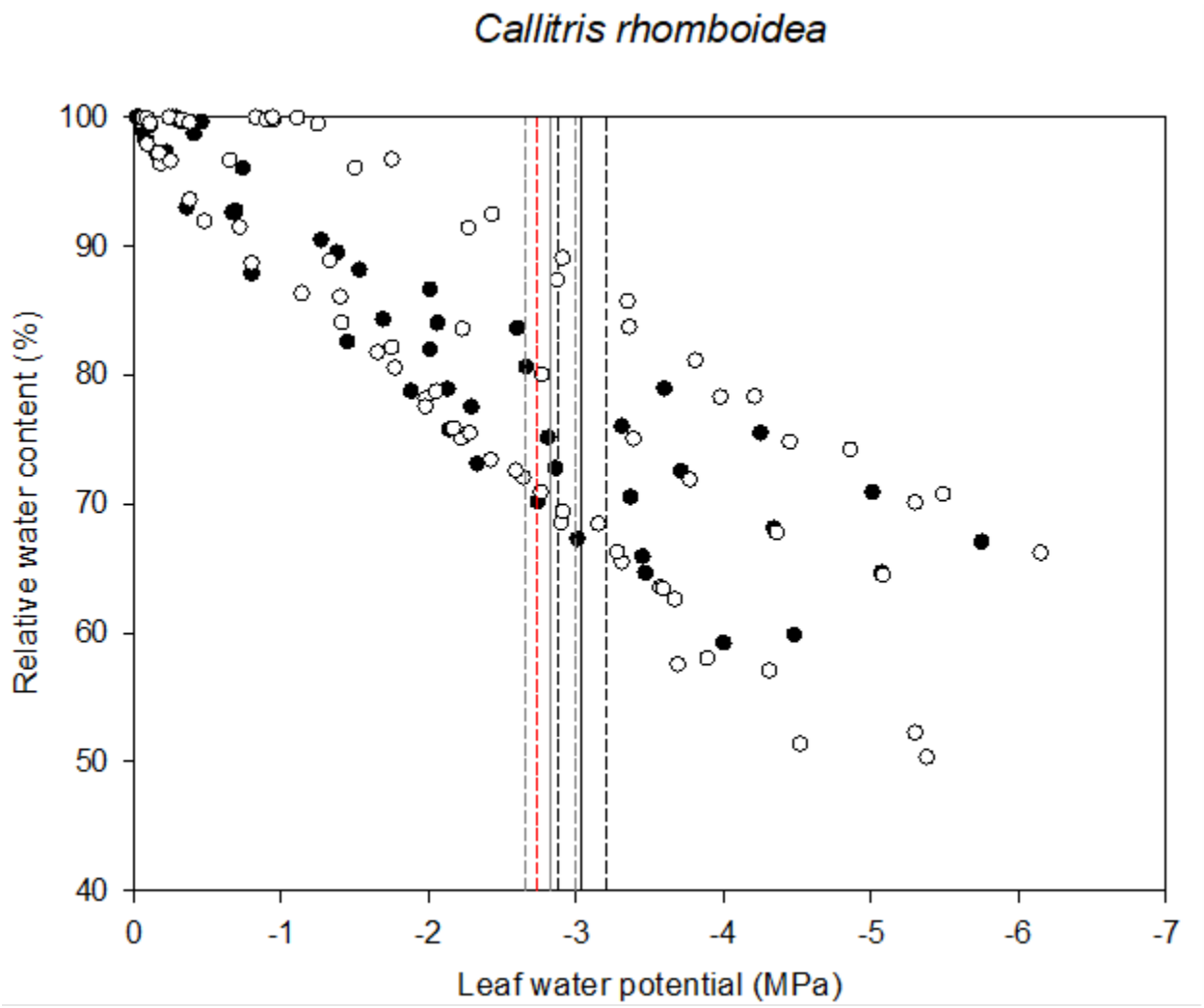

Figure 16. Relative water content as leaf water potential (Ψ_l) declines in shoots of the conifer *Callitris rhomboidea* (n=5) for never-before stressed plants and plants that had experienced long-term drought and at least 10 days at Ψ_l more negative than when peak foliage ABA level occurred (open and closed circles, respectively). Black vertical and dashed lines represent mean leaf water potential at turgor loss point Ψ_{tlp} and standard error for leaves collected from plants under long-term drought. Grey solid and dashed vertical lines represent mean Ψ_{tlp} and standard error for leaves of never-before stressed plants. Red dashed lines depict the Ψ_l at which peak foliage ABA levels occurred.

1.3.6 Conversion of foliage ABA to ABA-GE and export in the phloem is critical for normal peaking behavior in the conifer *C. rhomboidea*.

The level of foliage ABA-GE was measured in girdled and ungirdled leaves prior to drought, at peak foliage ABA levels, and at the lowest foliage ABA levels post-peak to assess the potential role of esterification and export in the phloem as the driver of peaking foliage ABA dynamics. In ungirdled branches of *C. rhomboidea*, ABA-GE levels rose to a mean of 78.96 µg g-1 FW in leaves in which foliage ABA levels had peaked, a significant increase from a mean of 1.57 µg g-1 FW in unstressed leaves ($P < 0.01$) (Figure 17). ABA-GE level in ungirdled branches then dropped to a mean 12.65 µg g-1 FW, which was similar to pre-stressed conditions ($p > 0.05$) (Figure 17). In contrast, ABA-GE levels in girdled branches rose much less from a mean of 0.66 µg g-1 FW in unstressed leaves to 5.51 µg g-1 FW in leaves with peak foliage ABA levels ($P > 0.05$) (Figure 17). Furthermore, in gridled branches the level of ABA-GE continued to increase to mean of 7.53 µg g-1 FW in leaves collected when foliage ABA levels were the lowest after the peak, this value was significantly higher than the levels in leaves that were unstressed and had peak foliage ABA levels ($P < 0.05$) (Figure 17).

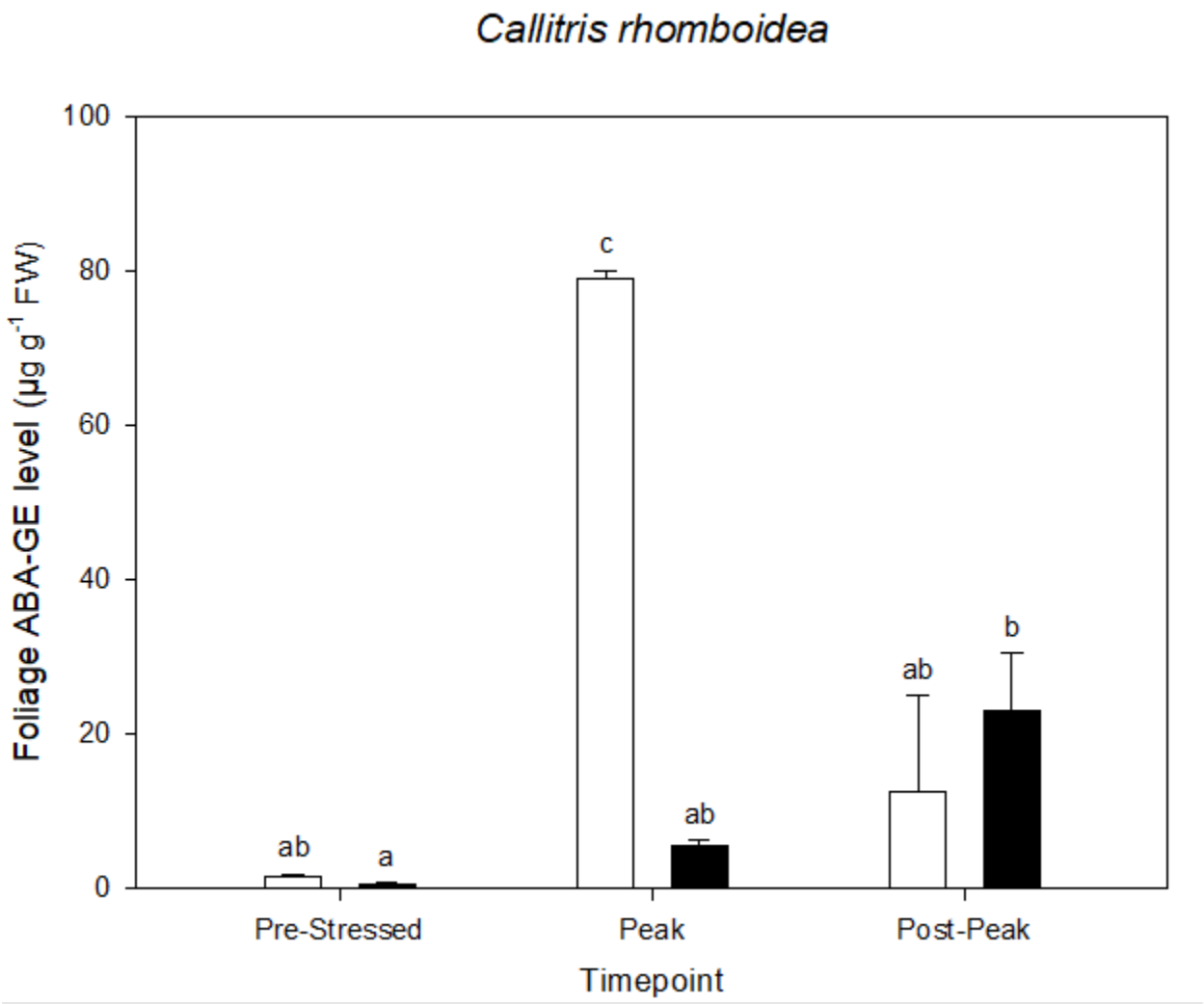

Figure 17. Mean foliage abscisic glucose ester (ABA-GE) levels at three different time points (pre-stressed leaves which were from unstressed plants prior to the drought, leaves that were at peak foliage ABA level during drought, and leaves that were at the lowest foliage ABA levels after the peak) in the conifer *Callitris romboidea* (n=3, ±SE). Bars and error bars represent mean ABA levels and standard error, respectively, for ungirdled (open bar) and girdled (closed bars) branches.

1.4 Discussion

In our study, we were able to demonstrate the occurrence of peaking type ABA dynamics in the angiosperm evergreen species *U. californica*. In *U. californica* levels of ABA during long term drought showed a highly similar pattern as leaf water potential declined to that of the classical model species that characterized peaking-type responses of ABA during long term drought, the conifer *C. rhomboidei* (Brodribb & McAdam, 2013). This result, coupled with previous reports of peaking type ABA dynamics in species from two genera in the Fabaceae family (Nolan et al., 2017; Yao, Li, et al., 2021; Yao, Nie, et al., 2021), all adapted to seasonally dry or arid environments and all with highly embolism resistant xylem, suggests that the evolution of the peaking type ABA response to long-term drought is linked to the evolution of highly resistant xylem, and is not just a conifer specific phenomenon. Highly resistant xylem has evolved frequently across angiosperm species suggesting that if the two are linked, highly embolism resistant xylem and the peaking type ABA dynamic, this ABA response to drought may quite commonly observed across angiosperms. Taken together our results demonstrate the occurrence of a peaking type ABA response now in two highly divergent angiosperm families the early diverging Lauraceae and the Fabaceae, future studies are needed to investigate whether this response is common across angiosperms with highly resistant xylem. The absence of high levels of ABA under long term drought suggest that, like in conifers, the stomata of these peaking type angiosperm species are closed passively by low water potentials under long term drought, this is a novel concept for stomatal biology, given that herbaceous ABA biosynthetic mutants have stomata that are generally insensitive to changes in leaf water status, which has suggested that passive regulation of stomatal aperture in response to changes in leaf water status are absent from this group of land plants.

The similarities in the dynamics of ABA levels during drought between the angiosperm species so far described and those of conifers, including the two species examined here, suggest

that there may be a shared mechanism driving the decline in ABA levels under long term drought stress across seed plants. By rapidly dehydrating branches on the bench that had been collected at two key timepoints (unstressed when ABA levels were low and once ABA levels had declined to a minimum during long term drought) we were able to assess the ability of both species to rapidly synthesize ABA in response to dehydration. This novel technique could allow us to study ABA biosynthetic capacity across a wide range of species without the need of sequencing key ABA biosynthetic genes as evidence for active ABA biosynthesis, which can be costly and time consuming and require prior genetic information. Our results show that ABA biosynthesis is highly active and rapid in unstressed branches that are rapidly dehydrated on the bench, but that this ability is eliminated in branches that are taken from plants when ABA levels are low under long-term drought and rehydrated overnight on the bench before dehydration.

These results illustrate that *de novo* ABA biosynthesis in response to dehydration ceases presumably after Ψ_{tlp} when ABA levels peak in each of the species. We believe that cessation of ABA biosynthesis at this point is the primary driver of declines in ABA levels under long-term drought, as the plant is no longer synthesizing ABA. Work still needs to be done to understand the mechanism behind deactivated ABA biosynthesis after Ψ_{tlp} and to confirm that indeed the expression of key ABA biosynthetic genes such as NCED are not upregulated on rapid dehydration in these branches that do not synthesize ABA. It is well known that as cells loose turgor ABA biosynthesis is triggered (Creelman & Mullet, 1991; Pereira & Pallardy, 1989; Pierce & Raschke, 1980), it could be that as the cell membrane separates from the wall on Ψ_{tlp} ABA biosynthesis stops. This could be due to cellular processes halting after loss of turgor or a physical disconnection causing a stop to membrane-wall interactions. Future studies in herbaceous species at Ψ_{tlp} for a certain time could elucidate the mechanism behind why ABA biosynthesis stops after Ψ_{tlp}.

However, these experiments could only be done in controlled environments since a slight decrease in water potential after tlp could cause cell death.

When ABA biosynthesis stops at Ψ_{tlp} our results suggest that a high export rate after conjugation of ABA into ABA-GE and not catabolism of the remaining is the main driver for ABA decline post peak once ABA biosynthesis ceases. It is believed that phloem flux is greatly reduced during drought (Epron et al., 2011; Hartmann, Ziegler, & Trumbore, 2013), however, our results from a girdling experiment in *C. rhomboidea* demonstrate a considerable reduction in the levels of ABA-GE post peak in ungirdled branches. This decline cannot be due to conversion of ABA-GE to ABA which is believed to be the way in which ABA-GE is itself catabolized, rather it is likely that this compound is exported in the phloem stream from the leaf very effectively. Evidence for this comes from a comparison of the ABA and ABA-GE dynamics in girdled branches in this species. We found that in girdled branches ABA dynamics during long-term drought were the same as ungirdled branches. Yet the accumulation of ABA-GE during long-term drought was highly divergent. Interestingly the levels of ABA-GE in girdled branches were lower than those of ungirdled branches, particularly at the peak time point of the ABA dynamic, suggesting that there might be tightly controlled feedback between ABA levels and ABA-GE conjugation rates. Early in a drought it seems that ABA biosynthesis is constantly active yet simultaneously there is a high rate of ABA conjugation to ABA-GE and then subsequently export from the leaf is occurring before cells loose turgor and after Ψ_{tlp}. Presumably this feedback allows ABA levels to be maintained at a certain threshold to keep stomata shut. This tight homeostatic regulation of ABA levels via conjugation rates to ABA-GE has not been previously described before. The evolution of highly resistant xylem allowed plants to have high safety margin and survive longer under decreasing negative water potentials (McAdam & Cardoso, 2019). The degree of safety margin

has been extensively studied and associated with the continuum of isohydric and anisohydric regulation. We know anisohydric regulation maintains gas exchange and photosynthesis to certain degree during drought and is correlated with high safety margin (McDowell et al., 2008; Sade, Gebremedhin, & Moshelion, 2012). This potentially provides an explanation for how ABA-GE export under long-term drought is still occurring even with a down regulation of phloem flux. We believe this to be the case across all species and suggest that peaking type dynamics is associated with anisohydric regulation.

By quantifying the levels of PA during long term drought, we were able to categorically rule out catabolism was a primary driver of a decrease in ABA levels after Ψ_{tlp}. Our results demonstrate that catabolism of ABA into PA did not significantly increase after peak ABA levels. Interestingly, the dynamic of PA levels and ABA levels during drought suggests that PA levels and the rate of ABA catabolism could be a simple function of current ABA level. Coupled with the increase in ABA-GE, the lack of a significant increase in PA levels at a certain water potential threshold suggest that the main mechanism of a decline in ABA levels is mainly due to export. Yet, future studies should also quantify upregulation of catabolism related genes during long term drought.

1.5 Conclusion

We successfully characterized the mechanism behind the peaking type response of ABA dynamics exhibited by highly drought tolerant species under long term drought (Figure 18). The use of rapid bench dehydration as an alternative method to assess ABA biosynthesis provided us with a powerful tool in the absence of available sequence genomes for species of interest, limiting research using modern molecular approaches. However, future work remains to be done to assess the occurrence of the peaking type behavior in a wider range of species across seed plants, including herbaceous species which usually die after a slight decrease in water potential after Ψ_{tlp}.

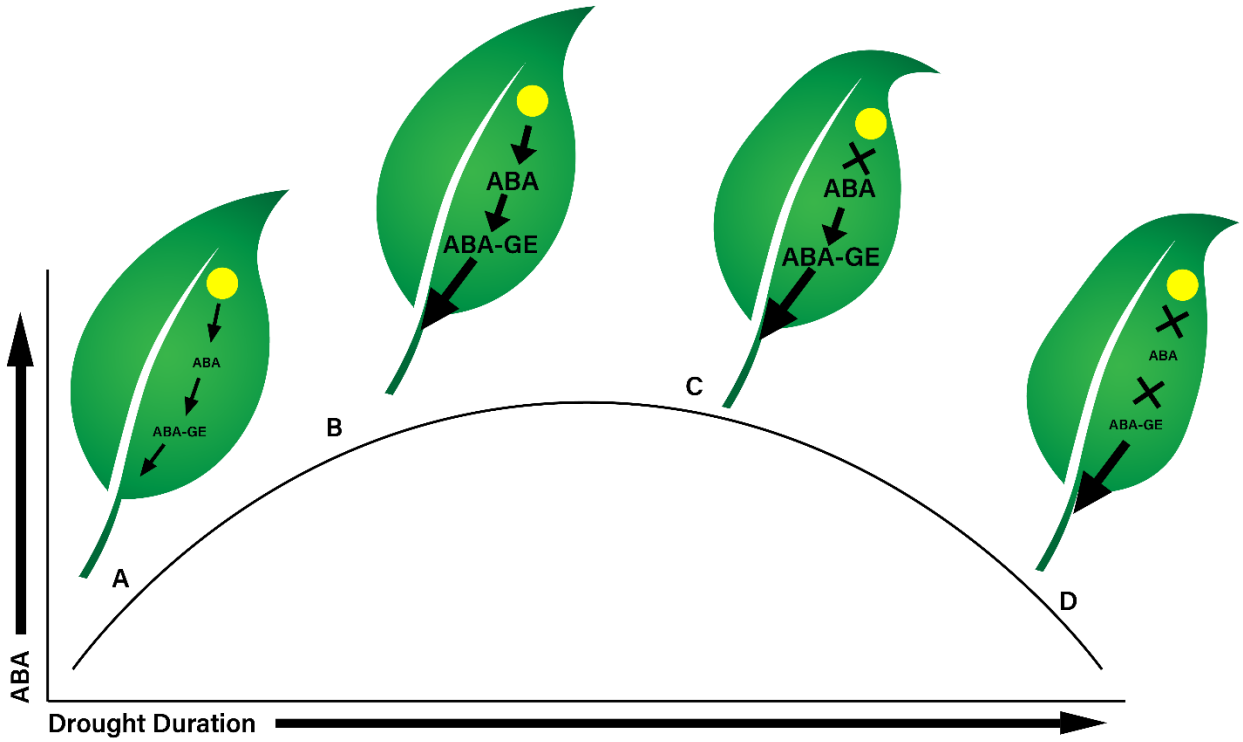

Figure 18. Schematic of the mechanism determining peaking type ABA dynamics in long-term drought. Early in drought (A) ABA biosynthesis rates and levels are low, thus levels of ABA-GE and export rates out of the leaf are low. As drought progresses (B), ABA level increases due to higher biosynthetic rates. At this point conversion of ABA to ABA-GE increases due to a higher pool of ABA and export of ABA-GE out of the leaves is also increased. After turgor loss point (C), ABA biosynthesis is shut down, ABA levels are still high, thus conversion to ABA-GE and export rate out of the leaf remain high. During later stages of drought (D), the ABA pool decreases as *de novo* biosynthesis remains inactive. Conversion to ABA-GE is reduced due to the diminished ABA pool size but export from the leaf still occurs which reduces ABA-GE levels. Yellow dots denote carotenoid precursor pools. Arrows from the precursor pool to ABA represent *de novo* ABA biosynthesis, arrows from ABA to ABA-GE represent esterification rates, and the arrow from ABA-GE to the petiole of the leaf represent ABA-GE export rate. The thickness of the arrows and size of the compound names represents the rate of the biochemical step or the relative level of the compound, respectively .

1.6 References

Bowles, A. M. C., Paps, J., & Bechtold, U. (2021). Evolutionary Origins of Drought Tolerance in Spermatophytes. *Frontiers in Plant Science*, *12*, 1068. https://doi.org/10.3389/fpls.2021.655924

Brodribb, T., Brodersen, C. R., Carriqui, M., Tonet, V., Rodriguez Dominguez, C., & McAdam, S. (2021). Linking xylem network failure with leaf tissue death. *New Phytologist*, *232*(1), 68–79. https://doi.org/10.1111/nph.17577

Brodribb, Tim J., & Cochard, H. (2009). Hydraulic failure defines the recovery and point of death in water-stressed conifers. *Plant Physiology*, *149*(1), 575–584. https://doi.org/10.1104/pp.108.129783

Brodribb, Timothy J., & McAdam, S. A. M. (2013). Abscisic acid mediates a divergence in the drought response of two conifers. *Plant Physiology*, *162*(3), 1370–1377. https://doi.org/10.1104/pp.113.217877

Brodribb, Timothy J., McAdam, S. A. M., Jordan, G. J., & Martins, S. C. V. (2014). Conifer species adapt to low-rainfall climates by following one of two divergent pathways. *Proceedings of the National Academy of Sciences of the United States of America*, *111*(40), 14489–14493. https://doi.org/10.1073/pnas.1407930111

Brodribb, Timothy J., Powers, J., Cochard, H., & Choat, B. (2020, April 17). Hanging by a thread? Forests and drought. *Science*. American Association for the Advancement of Science. https://doi.org/10.1126/science.aat7631

Cardoso, A. A., Randall, J. M., & McAdam, S. A. M. (2019). Hydraulics Regulate Stomatal Responses to Changes in Leaf Water Status in the Fern Athyrium filix-femina. *Plant Physiology*, *179*(2), 533–543. https://doi.org/10.1104/PP.18.01412

Castro, P., Puertolas, J., & Dodd, I. C. (2019). Stem girdling uncouples soybean stomatal conductance from leaf water potential by enhancing leaf xylem ABA concentration. *Environmental and Experimental Botany*, *159*, 149–156. https://doi.org/10.1016/J.ENVEXPBOT.2018.12.020

Chaves, M. M., Pereira, J. S., Maroco, J., Rodrigues, M. L., Ricardo, C. P. P., Osório, M. L., … Pinheiro, C. (2002). How plants cope with water stress in the field. Photosynthesis and growth. *Annals of Botany*, *89*(SPEC. ISS.), 907–916. https://doi.org/10.1093/aob/mcf105

Choat, B., Jansen, S., Brodribb, T. J., Cochard, H., Delzon, S., Bhaskar, R., … Zanne, A. E. (2012). Global convergence in the vulnerability of forests to drought. *Nature*, *491*(7426), 752–755. https://doi.org/10.1038/nature11688

Cochard, H., Pimont, F., Ruffault, J., & Martin-StPaul, N. (2020, May 11). SurEau.c: A mechanistic model of plant water relations under extreme drought. *BioRxiv*. bioRxiv. https://doi.org/10.1101/2020.05.10.086678

Creelman, R. A., & Mullet, J. E. (1991). Abscisic acid accumulates at positive turgor potential in excised soybean seedling growing zones. *Plant Physiology*, *95*(4), 1209–1213. https://doi.org/10.1104/pp.95.4.1209

Engelbrecht, B. M. J., Comita, L. S., Condit, R., Kursar, T. A., Tyree, M. T., Turner, B. L., & Hubbell, S. P. (2007). Drought sensitivity shapes species distribution patterns in tropical forests. *Nature*, *447*(7140), 80–82. https://doi.org/10.1038/nature05747

Epron, D., Ngao, J., Dannoura, M., Bakker, M. R., Zeller, B., Bazot, S., … Loustau, D. (2011). Seasonal variations of belowground carbon transfer assessed by in situ 13CO2 pulse labelling of trees. *Biogeosciences*, *8*(5), 1153–1168. https://doi.org/10.5194/BG-8-1153-2011

Han, Y., Watanabe, S., Shimada, H., & Sakamoto, A. (2020). Dynamics of the leaf endoplasmic reticulum modulate β-glucosidase-mediated stress-activated ABA production from its glucosyl ester. *Journal of Experimental Botany*, *71*(6), 2058–2071. https://doi.org/10.1093/jxb/erz528

Harris, M. J., & Dugger, W. M. (1986). The Occurrence of Abscisic Acid and Abscisyl-β-d-Glucopyranoside in Developing and Mature Citrus Fruit as Determined by Enzyme Immunoassay. *Plant Physiology*, *82*(2), 339–345. https://doi.org/10.1104/pp.82.2.339

Hartmann, H., Ziegler, W., & Trumbore, S. (2013). Lethal drought leads to reduction in nonstructural carbohydrates in Norway spruce tree roots but not in the canopy. *Functional Ecology*, *27*(2), 413–427. https://doi.org/10.1111/1365-2435.12046

Hetherington, A. M., & Woodward, F. I. (2003). The role of stomata in sensing and driving environmental change. *Nature*, *424*(6951), 901–908. https://doi.org/10.1038/nature01843

Hothorn, T., Bretz, F., & Westfall, P. (2008). Simultaneous inference in general parametric models. *Biometrical Journal. Biometrische Zeitschrift*, *50*(3), 346–363. https://doi.org/10.1002/BIMJ.200810425

Ikegami, K., Okamoto, M., Seo, M., & Koshiba, T. (2009). Activation of abscisic acid biosynthesis in the leaves of Arabidopsis thaliana in response to water deficit. *Journal of Plant Research*, *122*(2), 235–243. https://doi.org/10.1007/s10265-008-0201-9

Jeschke, W. D., Holobradá, M., & Hartung, W. (1997). Growth of Zea mays L. plants with their seminal roots only. Effects on plant development, xylem transport, mineral nutrition and the flow and distribution of abscisic acid (ABA) as a possible shoot to root signal. *Journal of Experimental Botany*, *48*(311), 1229–1239. https://doi.org/10.1093/jxb/48.6.1229

Jones, R. J., & Mansfield, T. A. (1970). Suppression of stomatal opening in leaves treated with abscisic acid. *Journal of Experimental Botany*, *21*(3), 714–719. https://doi.org/10.1093/JXB/21.3.714

Kerstiens, G. (1996). Cuticular water permeability and its physiological significance. *Journal of Experimental Botany*, *47*(12), 1813–1832. Retrieved from https://academic.oup.com/jxb/article/47/12/1813/545553

Larter, M., Pfautsch, S., Domec, J.-C., Trueba, S., Nagalingum, N., & Delzon, S. (2017). Aridity drove the evolution of extreme embolism resistance and the radiation of conifer genus Callitris. *New Phytologist*, *215*(1), 97–112. https://doi.org/10.1111/NPH.14545

Lim, E. K., Doucet, C. J., Hou, B., Jackson, R. G., Abrams, S. R., & Bowles, D. J. (2005). Resolution of (+)-abscisic acid using an Arabidopsis glycosyltransferase. *Tetrahedron Asymmetry*, *16*(1), 143–147. https://doi.org/10.1016/j.tetasy.2004.11.062

López, R., Brossa, R., Gil, L., & Pita, P. (2015). Stem girdling evidences a trade-off between cambial activity and sprouting and dramatically reduces plant transpiration due to feedback inhibition of photosynthesis and hormone signaling. *Frontiers in Plant Science*, *6*(APR), 285. https://doi.org/10.3389/FPLS.2015.00285/BIBTEX

Martin-StPaul, N., Delzon, S., & Cochard, H. (2017). Plant resistance to drought depends on timely stomatal closure. *Ecology Letters*, *20*(11), 1437–1447. https://doi.org/10.1111/ele.12851

McAdam, S. A. M. (2015). Physicochemical Quantification of Abscisic Acid Levels in Plant Tissues with an Added Internal Standard by Ultra-Performance Liquid Chromatography. *BIO-PROTOCOL*, *5*(18). https://doi.org/10.21769/bioprotoc.1599

Mcadam, S. A. M., & Brodribb, T. J. (2015). Hormonal dynamics contributes to divergence in seasonal stomatal behaviour in a monsoonal plant community. *Plant Cell and Environment*, *38*(3), 423–432. https://doi.org/10.1111/pce.12398

McAdam, S. A. M., & Brodribb, T. J. (2012). Fern and Lycophyte Guard Cells Do Not Respond to Endogenous Abscisic Acid. *The Plant Cell*, *24*(4), 1510–1521. https://doi.org/10.1105/TPC.112.096404

McAdam, S. A. M., & Brodribb, T. J. (2016). Linking turgor with ABA biosynthesis: Implications for stomatal responses to vapor pressure deficit across land plants. *Plant Physiology*, *171*(3), 2008–2016. https://doi.org/10.1104/pp.16.00380

McAdam, S. A. M., & Cardoso, A. A. (2019). The recurrent evolution of extremely resistant xylem. *Annals of Forest Science*, *76*(1), 1–4. https://doi.org/10.1007/s13595-018-0786-7

McAdam, S. A. M., Sussmilch, F. C., & Brodribb, T. J. (2015). Stomatal responses to vapour pressure deficit are regulated by high speed gene expression in angiosperms. *Plant Cell and Environment*, *39*(3), 485–491. https://doi.org/10.1111/pce.12633

McDowell, N., Pockman, W. T., Allen, C. D., Breshears, D. D., Cobb, N., Kolb, T., … Yepez, E. A. (2008, June). Mechanisms of plant survival and mortality during drought: Why do some plants survive while others succumb to drought? *New Phytologist*. https://doi.org/10.1111/j.1469-8137.2008.02436.x

Mitchell, P. J., McAdam, S. A. M., Pinkard, E. A., & Brodribb, T. J. (2017). Significant contribution from foliage-derived ABA in regulating gas exchange in Pinus radiata. *Tree Physiology*, *37*(2), 236–245. https://doi.org/10.1093/TREEPHYS/TPW092

Mittelheuser, C. J., & van Steveninck, R. F. M. (1969). Stomatal Closure and Inhibition of Transpiration induced by (RS)-Abscisic Acid. *Nature*, *221*, 281–282.

Mittelheuser, C. J., & van Steveninck, R. F. M. (1971). Rapid action of abscisic acid on photosynthesis and stomatal resistance. *Planta*, *97*(1), 83–86. https://doi.org/10.1007/BF00388408

Nolan, R. H., Tarin, T., Santini, N. S., McAdam, S. A. M., Ruman, R., & Eamus, D. (2017). Differences in osmotic adjustment, foliar abscisic acid dynamics, and stomatal regulation between an isohydric and anisohydric woody angiosperm during drought. *Plant Cell and Environment*, *40*(12), 3122–3134. https://doi.org/10.1111/pce.13077

Pereira, J. S., & Pallardy, S. (1989). Water Stress Limitations to Tree Productivity. In *Biomass Production by Fast-Growing Trees* (pp. 37–56). Springer, Dordrecht. https://doi.org/10.1007/978-94-009-2348-5_3

Pierce, M., & Raschke, K. (1980). Correlation between loss of turgor and accumulation of abscisic acid in detached leaves. *Planta*, *148*(2), 174–182. https://doi.org/10.1007/BF00386419

Pierce, M., & Raschke, K. (1981). Synthesis and metabolism of abscisic acid in detached leaves of Phaseolus vulgaris L. after loss and recovery of turgor. *Planta 1981 153:2*, *153*(2), 156–165. https://doi.org/10.1007/BF00384097

Priest, D. M., Ambrose, S. J., Vaistij, F. E., Elias, L., Higgins, G. S., Ross, A. R. S., … Bowles, D. J. (2006). Use of the glucosyltransferase UGT71B6 to disturb abscisic acid homeostasis in Arabidopsis thaliana. *Plant Journal*, *46*(3), 492–502. https://doi.org/10.1111/j.1365-313X.2006.02701.x

Qin, X., & Zeevaart, J. A. D. (1999). The 9-cis-epoxycarotenoid cleavage reaction is the key regulatory step of abscisic acid biosynthesis in water-stressed bean. *Proceedings of the National Academy of Sciences of the United States of America*, *96*(26), 15354–15361. https://doi.org/10.1073/pnas.96.26.15354

Rodriguez-Dominguez, C. M., Buckley, T. N., Egea, G., de Cires, A., Hernandez-Santana, V., Martorell, S., & Diaz-Espejo, A. (2016). Most stomatal closure in woody species under moderate drought can be explained by stomatal responses to leaf turgor. *Plant Cell and Environment*, *39*(9), 2014–2026. https://doi.org/10.1111/pce.12774

Sack, L., & PrometheusWiki contributors. (2010). Pressure-volume curves. Retrieved from /tiki-pagehistory.php?page=Pressure-volume curves&preview=4

Sade, N., Gebremedhin, A., & Moshelion, M. (2012). Risk-taking plants: anisohydric behavior as a stress-resistance trait. *Plant Signaling & Behavior*. https://doi.org/10.4161/psb.20505

Schindelin, J., Arganda-Carreras, I., Frise, E., Kaynig, V., Longair, M., Pietzsch, T., … Cardona, A. (2012, July). Fiji: An open-source platform for biological-image analysis. *Nature Methods*. Nat Methods. https://doi.org/10.1038/nmeth.2019

Sevanto, S. (2014). Phloem transport and drought. *Journal of Experimental Botany*, *65*(7), 1751–1759. https://doi.org/10.1093/JXB/ERT467

Skelton, R. P., Brodribb, T. J., & Choat, B. (2017). Casting light on xylem vulnerability in an herbaceous species reveals a lack of segmentation. *New Phytologist*, *214*(2), 561–569. https://doi.org/10.1111/NPH.14450

Tardieu, F., & Davies, W. J. (1992). Stomatal Response to Abscisic Acid Is a Function of Current Plant Water Status. *Plant Physiology*, *98*(2), 540–545. https://doi.org/10.1104/PP.98.2.540

Tombesi, S., Nardini, A., Frioni, T., Soccolini, M., Zadra, C., Farinelli, D., … Palliotti, A. (2015). Stomatal closure is induced by hydraulic signals and maintained by ABA in drought-stressed grapevine. *Scientific Reports*, *5*(1), 1–12. https://doi.org/10.1038/srep12449

Tyree, M. T., & Hammel, H. T. (1972). The measurement of the turgor pressure and the water relations of plants by the pressure-bomb technique. *Journal of Experimental Botany*, *23*(1), 267–282. https://doi.org/10.1093/jxb/23.1.267

Uknes, S. J., & Ho, T.-H. D. (1984). Mode of Action of Abscisic Acid in Barley Aleurone Layers. *Plant Physiology*, *75*(4), 1126–1132. https://doi.org/10.1104/pp.75.4.1126

Urli, M., Porté, A. J., Cochard, H., Guengant, Y., Burlett, R., & Delzon, S. (2013). Xylem embolism threshold for catastrophic hydraulic failure in angiosperm trees. *Tree Physiology*, *33*(7), 672–683. https://doi.org/10.1093/treephys/tpt030

Wood, S. N. (2011). Fast stable restricted maximum likelihood and marginal likelihood estimation of semiparametric generalized linear models. *Journal of the Royal Statistical Society: Series B (Statistical Methodology)*, *73*(1), 3–36. https://doi.org/10.1111/J.1467-9868.2010.00749.X

Xu, Z. Y., Lee, K. H., Dong, T., Jeong, J. C., Jin, J. B., Kanno, Y., … Hwang, I. (2012). A Vacuolar β-Glucosidase Homolog That Possesses Glucose-Conjugated Abscisic Acid Hydrolyzing Activity Plays an Important Role in Osmotic Stress Responses in Arabidopsis. *The Plant Cell*, *24*(5), 2184–2199. https://doi.org/10.1105/TPC.112.095935

Yao, G. Q., Li, F. P., Nie, Z. F., Bi, M. H., Jiang, H., Liu, X. D., … Fang, X. W. (2021). Ethylene, not ABA, is closely linked to the recovery of gas exchange after drought in four Caragana species. *Plant Cell and Environment*, *44*(2), 399–411. https://doi.org/10.1111/pce.13934

Yao, G. Q., Nie, Z. F., Turner, N. C., Li, F. M., Gao, T. P., Fang, X. W., & Scoffoni, C. (2021). Combined high leaf hydraulic safety and efficiency provides drought tolerance in Caragana species adapted to low mean annual precipitation. *New Phytologist*, *229*(1), 230–244. https://doi.org/10.1111/nph.16845

Zeevaart, J. A. D., & Boyer, G. L. (1984). Accumulation and Transport of Abscisic Acid and Its Metabolites in Ricinus and Xanthium. *Plant Physiology*, *74*(4), 934–939. https://doi.org/10.1104/pp.74.4.934

Zhang, F.-P., Sussmilch, F., Nichols, D. S., Cardoso, A. A., Brodribb, T. J., & Mcadam, S. A. M. (2018). Leaves, not roots or floral tissue, are the main site of rapid, external pressure-induced ABA biosynthesis in angiosperms. *Journal of Experimental Botany*, *69*(5), 1261–1267. https://doi.org/10.1093/jxb/erx480